



UNIVERSITY OF LEEDS

This is a repository copy of *NEXMD v2.0 Software Package for Nonadiabatic Excited State Molecular Dynamics Simulations*.

White Rose Research Online URL for this paper:

<https://eprints.whiterose.ac.uk/202875/>

Version: Accepted Version

---

**Article:**

Freixas, V.M. [orcid.org/0000-0003-1733-4827](https://orcid.org/0000-0003-1733-4827), Malone, W. [orcid.org/0000-0001-8245-322X](https://orcid.org/0000-0001-8245-322X), Li, X. [orcid.org/0000-0001-8666-0138](https://orcid.org/0000-0001-8666-0138) et al. (17 more authors) (2023) NEXMD v2.0 Software Package for Nonadiabatic Excited State Molecular Dynamics Simulations. *Journal of Chemical Theory and Computation*, 19 (16). pp. 5356-5368. ISSN 1549-9618

<https://doi.org/10.1021/acs.jctc.3c00583>

---

© 2023 American Chemical Society. This is an author produced version of an article published in *Journal of Chemical Theory and Computation*. Uploaded in accordance with the publisher's self-archiving policy.

**Reuse**

Items deposited in White Rose Research Online are protected by copyright, with all rights reserved unless indicated otherwise. They may be downloaded and/or printed for private study, or other acts as permitted by national copyright laws. The publisher or other rights holders may allow further reproduction and re-use of the full text version. This is indicated by the licence information on the White Rose Research Online record for the item.

**Takedown**

If you consider content in White Rose Research Online to be in breach of UK law, please notify us by emailing [eprints@whiterose.ac.uk](mailto:eprints@whiterose.ac.uk) including the URL of the record and the reason for the withdrawal request.



[eprints@whiterose.ac.uk](mailto:eprints@whiterose.ac.uk)  
<https://eprints.whiterose.ac.uk/>

# NEXMD v2.0 Software Package for Nonadiabatic Excited State Molecular Dynamics Simulations

Victor M. Freixas,<sup>a</sup> Walter Malone,<sup>b</sup> Xinyang Li,<sup>c</sup> Huajing Song,<sup>c</sup> Hassiel Negrin-Yuvero,<sup>d</sup> Royle Pérez-Castillo,<sup>d</sup> Alexander White,<sup>c</sup> Tammie R. Gibson,<sup>c</sup> Dmitry V. Makhov,<sup>e,f</sup> Dmitrii V. Shalashilin,<sup>c</sup> Yu Zhang,<sup>c</sup> Nikita Fedik,<sup>c</sup> Maksim Kulichenko,<sup>c</sup> Richard Messerly,<sup>c</sup> Luke Nambi Mohanam,<sup>g</sup> Sahar Sharifzadeh,<sup>g</sup> Adolfo Bastida,<sup>h</sup> Shaul Mukamel,<sup>a</sup> Sebastian Fernandez-Alberti,<sup>d</sup> Sergei Tretiak<sup>c</sup>

<sup>a</sup>*Departments of Chemistry and Physics and Astronomy, University of California, Irvine, California 92697-2025, USA*

<sup>b</sup>Department of Physics, Tuskegee University, Tuskegee, AL 36088, USA

<sup>c</sup>Theoretical Division, Center for Nonlinear Studies (CNLS), and Center for Integrated Nanotechnologies (CINT), Los Alamos National Laboratory, Los Alamos, NM 87545, USA

<sup>d</sup>Departamento de Ciencia y Tecnología, Universidad Nacional de Quilmes/CONICET, B1876BXD Bernal, Argentina

<sup>e</sup>School of Chemistry, University of Leeds, Leeds LS2 9JT, United Kingdom

<sup>f</sup>School of Mathematics, University of Bristol, Bristol BS8 1TW, United Kingdom

<sup>g</sup>Department of Electrical and Computer Engineering, College of Engineering, Boston University, MA 02215, USA

<sup>h</sup>Departamento de Química Física, Universidad de Murcia, Murcia 30100, Spain.

## Abstract

We present NEXMD v2.0, the second release of the NEXMD (Nonadiabatic EXcited-state Molecular Dynamics) software package. Across a variety of new features, NEXMD v2.0 incorporates new implementations of two hybrid quantum-classical dynamics methods, namely Ehrenfest dynamics (EHR) and the Ab-Initio Multiple Cloning sampling technique for Multiconfigurational Ehrenfest quantum dynamics (MCE-AIMC or simply AIMC), which are alternative options to the previously implemented trajectory surface hopping (TSH) method. To illustrate these methodologies, we outline a direct comparison of these three hybrid quantum-classical dynamics methods as implemented in the same NEXMD framework, discussing their weaknesses and strengths; using the modelled photodynamics of a polyphenylene ethylene dendrimer building block as a representative example. We also describe the expanded normal mode analysis and constraints for both the ground and excited states, newly implemented in the NEXMD v2.0 framework, which allow for a deeper analysis of the main vibrational motions involved in vibronic dynamics. Overall, NEXMD v2.0 expands the range of applications of NEXMD to a larger variety of multichromophore organic molecules and photophysical processes involving quantum coherences and/or persistent couplings between electronic excited states and nuclear velocity.

## 1. Introduction

In the last few decades, a great volume of research has focused on the discovery and design of new materials with desired photoactive properties. Inspiring examples in nature, such as vision<sup>1</sup> and photosynthesis,<sup>2-4</sup> have brought to the spotlight organic conjugated materials ranging from small molecules and donor-acceptor systems to polymers and molecular crystals.<sup>5,6</sup> These systems feature complex excited state electronic structure arising from strong electronic correlations and low dimensionality,<sup>7</sup> combined with delocalized and polarizable  $\pi$ -electrons that are key for the generation of mobile charge carriers.<sup>6</sup> Such systems typically undergo an efficient non-radiative relaxation<sup>8</sup> that can take place through several nonadiabatic pathways leading to overall dissipation of an excess of electronic energy into heat. Many physical processes, such as internal conversion,<sup>9</sup> energy transfer,<sup>10</sup> charge separation,<sup>11,12</sup> exciton self-trapping<sup>13</sup> or vibronic coherences,<sup>14-16</sup> can be important. While the development of novel synthesis procedures has opened a wide range of materials design possibilities, computational methods have arisen alongside as an essential tool to facilitate such explorations by lowering the cost of the experimental trial-and-error approach. These computational methods provide atomistic insights and the electronic structure features responsible for the functionality of various devices, such as organic light emitting diodes,<sup>17</sup> photovoltaics,<sup>18-20</sup> field-effect transistors,<sup>21,22</sup> sensors,<sup>23-27</sup> photocatalysts<sup>28</sup> or solar cells.<sup>29,30</sup> Consequently, multiple software packages have been developed for performing nonadiabatic molecular dynamics (NAMD) simulations, such as Q-Chem,<sup>31</sup> SHARC,<sup>32-34</sup> COBRAMM,<sup>35</sup> Newton-X,<sup>36,37</sup> PYXAID,<sup>38,39</sup> NWChem,<sup>40-42</sup> TURBOMOLE,<sup>43,44</sup> *Libra*,<sup>45</sup> *PyUNIxMD*,<sup>46</sup> *DynEmol*,<sup>47</sup> *JADE*,<sup>48</sup> *Hefei-NAMD*,<sup>49</sup> and NEXMD.<sup>50,51</sup>

In particular, NEXMD<sup>50</sup> (Nonadiabatic EXcited-state Molecular Dynamics) has been aimed to describe photoinduced phenomena in relatively large conjugated molecular systems. In this paper, we present the next release of the package, NEXMD **v2.0**, which incorporates implementations of additional methods that enable computational modeling of a larger variety of multichromophore organic molecules and photophysical processes involving quantum coherences and/or persistent couplings between electronic excited states. NEXMD can perform both Born-Oppenheimer Molecular Dynamics (BOMD) and Non-Adiabatic Molecular Dynamics (NAMD). The original NEXMD release was limited to using only the Fewest Switches Trajectory Surface Hopping (TSH)<sup>52</sup> algorithm for NAMD, with an adiabatic basis set to represent quantum transitions through the manifold of excited states. NEXMD **v2.0** now also incorporates alternative NAMD methods, namely, Ehrenfest dynamics (EHR)<sup>53</sup> and the Ab-Initio Multiple Cloning (AIMC)<sup>54</sup> sampling technique for Multiconfigurational Ehrenfest quantum dynamics (MCE).<sup>55</sup> As implemented in NEXMD **v2.0**, all three methods (i.e., TSH, EHR, AIMC) share the same level of electronic structure implementation consisting of Configuration Interaction Singles (CIS)<sup>56</sup> or Time-Dependent Hartree-Fock (TDHF)<sup>57,58</sup> combined with semiempirical Hamiltonian models. The latter provides a fast and sufficiently accurate description of the excited state manifold for molecules in the range of one to three hundred atoms and including up to a few dozen excited states. Furthermore, analytical routines allow on-the-fly calculation of excited states nonadiabatic couplings<sup>59,60</sup> and gradients.<sup>61-63</sup> The combination of these features has allowed the application of NEXMD to study a broad range of materials including polymers,<sup>64-70</sup> dendrimers,<sup>16,71-77</sup> nanorings and nanobelts,<sup>78-83</sup> light harvesting complexes<sup>2,3,84</sup> and energetic materials.<sup>85-87</sup>

The paper is organized as follows. Section 2 covers the new features released in NEXMD **v2.0**, highlighting in particular the theory behind the new available nonadiabatic molecular dynamics methods, i.e. EHR and AIMC. In Section 3 we present exemplary simulations of the photoinduced dynamics of a polyphenylene ethylene (PPE) dendrimer building block emphasizing

the effects of different new features implemented in NEXMD v2.0. Finally, in Section 4 we present our concluding remarks and perspectives of future implementations.

## 2. NEXMD/NEXMD v2.0 features

NEXMD/NEXMD v2.0 have been developed to perform on-the-fly ground-state, and adiabatic or non-adiabatic excited state molecular dynamics simulations at Hartree Fock (HF), and TDHF, or CIS levels of electronic structure using semiempirical Hamiltonians. The abbreviated list of features released in NEXMD v2.0 compared to NEXMD are given in Table I. All of them have been tested in previous articles<sup>14–16,76,88–90</sup> and they we are finally getting release in NEXMD v2.0.

**Table I.** Features present in NEXMD/NEXMD v2.0.

Features	NEXMD	NEXMD v2.0
Semiempirical Hamiltonian models (AM1, MNDO, PM3, PM6)	✓	✓
Hartree Fock ground state	✓	✓
TDHF or CIS excited states	✓	✓
Continuum solvation models	✓	✓
Analytical ground and excited-state gradients	✓	✓
Analytical non-adiabatic couplings	✓	✓
Geometry optimization of ground or excited states	✓	✓
Langevin thermostat	✓	✓
Adiabatic dynamics of ground or excited states	✓	✓
Trajectory Surface Hopping NAMD	✓	✓
Empirical decoherence methods	✓	✓
Trivial unavoided crossings	✓	✓
On-the-fly elimination of unnecessary states		✓
Ehrenfest NAMD		✓
Ab-Initio Multiple Cloning sampling technique for Multiconfigurational Ehrenfest NAMD		✓
Hessian and vibrational normal modes calculations		✓
Distance constraints (RATTLE) for dynamics		✓
Normal modes constraints (FrozeNM) for dynamics		✓
Orbital analysis of transition density	✓	✓
Analysis of transition density flux	✓	✓
Real space analysis of transition density matrix	✓	✓

### 2.1 *Electronic structure calculation overview*

While the detailed NEXMD electronic structure calculation background can be found elsewhere,<sup>50</sup> we briefly summarize it here for the sake of completeness. The ground state density matrix is calculated with the means of the Hartree Fock (HF) self-consistent field iterative procedure.<sup>56</sup> NEXMD utilizes semiempirical quantum mechanics **methods**,<sup>91</sup> including several

semiempirical Hamiltonians including the Austin Model (AM1),<sup>92</sup> the Parametrized Model 3 (PM3)<sup>93</sup> and the Parametrized Model 6 (PM6),<sup>94</sup> among others.

The time-dependent Hartree–Fock (TDHF) equation is solved for the single electron transition density matrix<sup>95</sup> using the Collective Electronic Oscillator (CEO) approach.<sup>96,97</sup> A single electron transition density matrix element, representing a transition from the ground state (denoted as 0) to an excited state  $I$ , is given by:

$$(\rho_{0I})_{nm} = \langle \phi_0 | c_m^\dagger c_n | \phi_I \rangle, \quad (1)$$

Where  $c_m^\dagger$  and  $c_n$  are the electronic creation and annihilation operators acting over the atomic orbitals  $m$  and  $n$ , respectively. These transition density matrices are the eigenfunctions of the Liouville superoperator  $L$ ,<sup>98</sup> or in tetradic notation:

$$L\xi_I = \Omega_I \xi_I, \quad (2)$$

Where  $\xi_I$  is the transition density matrix  $\rho_{0I}$  spanned as a column vector and  $\Omega_I$  is the transition energy from the ground state to excited state  $I$ . In the molecular orbital basis, this equation can be recast in the form:<sup>63</sup>

$$\begin{pmatrix} A & B \\ -B & -A \end{pmatrix} \begin{bmatrix} X \\ Y \end{bmatrix} = \Omega \begin{bmatrix} X \\ Y \end{bmatrix}, \quad (3)$$

which is also known as the Random Phase Approximation (RPA) eigenvalue equation.<sup>56</sup> In this representation, transition density matrices  $\xi = \begin{bmatrix} X \\ Y \end{bmatrix}$  consist of particle-hole  $X$  and hole-particle  $Y$  subparts.<sup>96</sup> Neglecting the nondiagonal blocks  $B$  is equivalent to the CIS approximation,<sup>99</sup> analogue to the Tamm-Dancoff approximation,<sup>100</sup> leading to:

$$AX = \Omega X, \quad (4)$$

Where  $A$  is the Hermitian CIS matrix. TDHF includes the calculation of  $B$ , making it computationally more expensive. For both cases, solving for every eigenfunction is too expensive. Instead, the Davidson diagonalization algorithm<sup>99,101–103</sup> is used to find numerically converging solutions for the requested number of the lowest energy excited states. For practical purpose, two additional states beyond the requested number are always computed with the Davidson algorithm, since the algorithm is empirically known to occasionally energetically mis-order two states in the iterative diagonalization procedure leading to ‘skipped’ states. The number of eigenfunctions requested determines the size of the adiabatic electronic basis for NAMD.

## 2.2 Nonadiabatic molecular dynamics methods

NEXMD v2.0 has three different methods to perform nonadiabatic excited-state molecular dynamics on-the-fly: TSH, EHR, and MCE coupled with AIMC. TSH dynamics has already been extensively explored<sup>104</sup> and applied to a wide range of photophysical processes.<sup>105–107</sup> In general, EHR dynamics is adequate for homogeneous dynamic processes involving weak, but persistent, couplings between electronic excited states.<sup>15,108</sup> However, in contrast to TSH, EHR cannot

describe branching relaxation pathways, transient population trapping on specific electronic states, or electronic relaxations involving state-specific driving forces. Furthermore, both TSH and EHR dynamics suffer from improper treatment of decoherence in the electronic system. MCE treats decoherence in a natural way beyond mean-field Born-Oppenheimer dynamics on several excited states, expanding the range of practical applications.<sup>14,16,42,109</sup> The implementation of these three methods within the NEXMD framework allows for a direct comparison of their weaknesses and strengths,<sup>88</sup> as well as their relative efficiencies. Taking TSH as reference, which is the fastest, EHR dynamics can be approximately ***n* times fold slower, where *n* is the number of excited states considered**, typically from 2 to 10. For a larger number of states, EHR dynamics becomes impractical because all gradients for states and coupling between pairs of states are required. While being a controlled approximation, AIMC adds an extra numerical cost: each bifurcation augments the nuclear basis set with a new configuration coming with its own electronic structure. Depending on the number of clones, AIMC dynamics can be approximately one order of magnitude slower than EHR dynamics.

### 2.2.1 Ehrenfest (EHR) dynamics

In the NEXMD **v2.0** implementation of EHR dynamics, nuclei are treated classically while the electronic wave function is expanded over  $N_I$  adiabatic states,  $\phi_I$ :

$$\varphi = \sum_I^{N_I} a_I \phi_I. \quad (5)$$

The coefficients  $a_I$  evolve in time according to:<sup>110</sup>

$$\dot{a}_I = -\frac{i}{\hbar} V_I - \sum_J a_J \dot{\mathbf{R}} \cdot \mathbf{d}_{IJ}, \quad (6)$$

Where  $V_I$  is the electronic potential energy of the excited state  $I$ ,  $\dot{\mathbf{R}}$  is the nuclear velocity and  $\mathbf{d}_{IJ}$  is the nonadiabatic coupling vector:

$$\mathbf{d}_{IJ} = \langle \phi_I | \nabla_{\mathbf{R}} | \phi_J \rangle, \quad (7)$$

With  $\nabla_{\mathbf{R}}$  being the gradient with respect to the nuclear coordinates  $\mathbf{R}$ . In this context, the force  $\mathbf{F}$  acting over the nuclei is given by:

$$\mathbf{F} = - \sum_I |a_I|^2 \nabla_{\mathbf{R}} V_I - \sum_{I,J} (a_J)^* a_I \mathbf{d}_{IJ} (V_I - V_J), \quad (8)$$

such that  $\mathbf{F}$  includes two terms: the first term corresponds to a sum of gradients for all electronic states weighted by their Ehrenfest populations  $|a_I|^2$  and the second term represents the nonadiabatic contribution. The quantities  $V_I$ ,  $\nabla_{\mathbf{R}} V_I$  and  $\mathbf{d}_{IJ}$  ( $I, J \leq N_I$ ) are calculated analytically on-the-fly at the electronic structure level described in Section 2.1.

### 2.2.2 Trajectory Surface Hopping (TSH) dynamics.

The TSH implementation also involves equations (5-7) but the nuclei evolve on a potential energy surface which is defined by a single electronic state at a given time. That is, the force acting over nuclei is reduced to:

$$F = -\nabla_{\mathbf{R}} V_I, \quad (9)$$

Stochastic hops from one electronic surface to another follow the Fewest Switches Surface Hopping (FSSH) prescription<sup>110</sup> and are governed by changes in the coefficients of the electronic wave function (eq. 6).<sup>52</sup> This original TSH method is implemented in NEXMD<sup>111</sup> and NEXMD v2.0 and several empirical schemes for corrections for decoherence<sup>112</sup> in the TSH approach can be used. Both EHR and TSH make use of the Min-Cost algorithm<sup>113</sup> to correct for trivial unavoided crossings.

### 2.2.3 MCE dynamics

MCE is a natural generalization of Ehrenfest dynamics. In the MCE approach, individual EHR trajectories guide Gaussian basis functions (a.k.a., configurations)  $\varphi_n$ <sup>55</sup>, which form the basis for the molecular wave function  $\Psi$ . Each configuration includes a single nuclear term  $\chi_n$  and a sum of electronic wavefunctions  $\phi_I^{(n)}$ .

$$\Psi = \sum_n c_n \varphi_n = \sum_n c_n \chi_n \sum_I a_I^{(n)} \phi_I^{(n)}, \quad (10)$$

The nuclear terms are coherent states (CS),<sup>55</sup> i.e. minimum uncertainty wave packets, which in the coordinate representation are frozen Gaussian functions centered over an Ehrenfest trajectory  $\mathbf{R}_n(t)$ ,  $\mathbf{P}_n(t)$ :

$$\chi_n = \left(\frac{2\alpha}{\hbar}\right)^{\frac{N_{DOF}}{4}} \exp\left(-\alpha(\mathbf{R} - \mathbf{R}_n(t))^2 + \frac{i}{\hbar} \mathbf{P}_n(t)(\mathbf{R} - \mathbf{R}_n(t)) + \frac{i}{\hbar} \gamma_n\right), \quad (11)$$

where  $\alpha$  is the Gaussian CS width depending on the type of atom,<sup>114</sup>  $N_{DOF}$  is the number of degrees of freedom,  $\mathbf{P}_n$  is the nuclear momentum and  $\gamma_n$  is a phase of the nuclear part which is propagated semiclassically according to:

$$\dot{\gamma}_n = \frac{\mathbf{P}_n \dot{\mathbf{R}}_n}{2}, \quad (12)$$

The electronic part of the molecular wave function  $\sum_I a_I^{(n)} \phi_I^{(n)}$  is represented in the Time-Dependent Diabatic Basis (TDDB).<sup>53</sup> The electronic wave functions  $\phi_I^{(n)}$  are calculated at the center  $\mathbf{R}_n$  of the  $n^{\text{th}}$  Gaussian CS (11) and implicitly depend on time due to the time dependence of  $\mathbf{R}_n$ . In TDDB, nonadiabatic couplings between electronic states originate from this time dependence, which is different from the Born-Huang approach,<sup>115</sup> where coupling between

electronic states originates from their parametric dependence on electronic coordinates. Nevertheless, the TDDB equations for coupled amplitudes  $a_i^{(n)}$  are the same as those obtained in an adiabatic Born-Huang basis (Eqs. 5-6).

The time evolution of complex amplitudes  $c_n$  is calculated on-the-fly by the time dependent Schrödinger equation:

$$\sum_n \langle \varphi_m | \varphi_n \rangle \dot{c}_n = -\frac{i}{\hbar} \sum_n \left( H_{mn} - i\hbar \left\langle \varphi_m \left| \frac{d\varphi_n}{dt} \right. \right\rangle \right) c_n, \quad (13)$$

where:

$$H_{mn} = \sum_{I,J} (a_J^{(m)})^* a_I^{(n)} \langle \chi_m \phi_J^{(m)} | (\hat{T} + \hat{V}) | \chi_n \phi_I^{(n)} \rangle, \quad (14)$$

and

$$\begin{aligned} \left\langle \varphi_m \left| \frac{d\varphi_n}{dt} \right. \right\rangle &= \left\langle \chi_m \left| \frac{d\chi_n}{dt} \right. \right\rangle \sum_{I,J} \langle \phi_J^{(m)} | \phi_I^{(n)} \rangle (a_J^{(m)})^* a_I^{(n)} \\ &\quad - \frac{i}{\hbar} \langle \chi_m | \chi_n \rangle \sum_{I,J} \langle \phi_J^{(m)} | \phi_I^{(n)} \rangle (a_J^{(m)})^* a_I^{(n)} V_I^{(n)}, \end{aligned} \quad (15)$$

where the first term depends on the matrix elements of the time derivative operator acting in the nuclear subspace and the second term was deduced taking into account the time dependent Schrödinger equation for the adiabatic expansion of the electronic wavefunction given by equation (5). The kinetic and potential matrix elements in equation (14) are evaluated as:

$$\langle \chi_m \phi_J^{(m)} | \hat{T} | \chi_n \phi_I^{(n)} \rangle = \langle \phi_J^{(m)} | \phi_I^{(n)} \rangle \left\langle \chi_m \left| -\frac{\hbar^2}{2} \nabla_R M^{-1} \nabla_R \right| \chi_n \right\rangle, \quad (16)$$

and:

$$\begin{aligned} &\langle \chi_m \phi_J^{(m)} | \hat{V} | \chi_n \phi_I^{(n)} \rangle \\ &= \frac{1}{2} \langle \phi_J^{(m)} | \phi_I^{(n)} \rangle \langle \chi_m | \chi_n \rangle \left\{ \left( V_J^{(m)} + V_I^{(n)} \right) + \frac{i}{4\alpha\hbar} (\mathbf{P}_n - \mathbf{P}_m) \right. \\ &\quad \left. \cdot \left( \nabla_R V_J^{(m)} + \nabla_R V_I^{(n)} \right) - \frac{1}{2} (\mathbf{R}_n - \mathbf{R}_m) \cdot \left( \nabla_R V_I^{(n)} - \nabla_R V_J^{(m)} \right) \right\}, \end{aligned} \quad (17)$$

where equation (16) is exact, while equation (17) utilizes the first-order averaged Taylor expansion of the potential energy.<sup>116</sup> The first-order linear interpolation of (17) does not involve any additional computational cost as the electronic energies and gradients were calculated to propagate the trajectories  $\mathbf{R}_n(t)$ ,  $\mathbf{P}_n(t)$  and  $\mathbf{R}_m(t)$ ,  $\mathbf{P}_m(t)$  of Gaussian CSs (11). All nuclear matrix elements  $\langle \chi_m | \chi_n \rangle$  and  $\left\langle \chi_m \left| \frac{d\chi_n}{dt} \right. \right\rangle$  can be calculated analytically<sup>116</sup> and the electronic overlaps are calculated on-the-fly according to:

$$\frac{d}{dt} \langle \phi_J^{(m)} | \phi_I^{(n)} \rangle = \sum_K \langle \phi_K^{(m)} | \phi_I^{(n)} \rangle \dot{\mathbf{R}}_m \cdot \mathbf{d}_{KJ}^{(m)} + \sum_K \langle \phi_J^{(m)} | \phi_K^{(n)} \rangle \dot{\mathbf{R}}_n \cdot \mathbf{d}_{KI}^{(n)}, \quad (18)$$

For the MCE method, the calculation of the expectation value of any operator includes contributions from all configurations and crossed terms between configurations. For example, the expectation value of the electronic populations is given by:<sup>54</sup>

$$\langle \hat{P}_K \rangle = \sum_{n,m} c_m^* c_n \langle \chi_m | \chi_n \rangle (a_K^{(m)})^* \sum_{I,J} a_I^{(n)} \langle \phi_K^{(m)} | \phi_I^{(n)} \rangle, \quad (19)$$

The sum of electronic populations over  $K$  (eq. 19) is the norm of the molecular wave function  $\Psi$  and should always equal to unity. This property can be used to check the numerical integration scheme. Another example of an observable expectation value is the fraction of transition density localized over a fragment of the molecule, expressed as:

$$\langle \hat{\rho}_X \rangle = \sum_{n,m} c_m^* c_n \langle \chi_m | \chi_n \rangle \sum_{I,J} (a_J^{(m)})^* a_I^{(n)} \langle \phi_K^{(m)} | \phi_I^{(n)} \rangle \rho_{I,X}^{(m)}, \quad (20)$$

where  $\rho_{I,X}^{(m)}$  is the fraction of transition density localized over the fragment  $X$  of the molecule for the excited state  $I$  in the centroid of configuration  $m$ .<sup>54</sup>

#### 2.2.4 AIMC sampling technique

EHR dynamics is meaningful only when the nuclei experience similar forces across all populated electronic states included in the calculation. Otherwise, the average EHR force lacks physical significance and configurations  $\varphi_n$  likely fail to explore dynamically important regions of the configurational space. AIMC is a sampling technique for MCE that overcomes this problem allowing bifurcations of the wave packet in a similar fashion to the Ab-Initio Multiple Spawning method,<sup>117,118</sup> therefore increasing of the number of configurations. After a bifurcation or *cloning event*, a configuration  $\varphi_n$ :

$$\varphi_n = \chi_n \sum_I a_I^{(n)} \phi_I^{(n)}, \quad (21)$$

is replaced by two new configurations (i.e., clones)  $\varphi_{n_1}$  and  $\varphi_{n_2}$  having the same nuclear components but different electronic distributions. One of these new configurations (or clones) will be subsequently propagated starting from a pure electronic excited state  $M$ :

$$\varphi_{n_1} = \chi_n \left( \frac{a_M^{(n)}}{|a_M^{(n)}|} \times \phi_I^{(n)} + \sum_{J \neq M} 0 \times \phi_J^{(n)} \right), \quad (22)$$

while the other configuration will continue propagating on a mixture of the remaining electronic states:

$$\varphi_{n_2} = \chi_n \left( 0 \times \phi_M^{(n)} + \frac{1}{\sqrt{1 - |a_M^{(n)}|^2}} \sum_{J \neq M} a_J^{(n)} \times \phi_J^{(n)} \right), \quad (23)$$

The excited state  $M$  is chosen to be the state having the greatest population just before the cloning point. The corresponding new nuclear amplitudes are set to:

$$c_{n_1} = c_n |a_M^{(n)}|, \quad (24)$$

and:

$$c_{n_2} = c_n \sqrt{1 - |a_M^{(n)}|^2}, \quad (25)$$

In this way, the continuity of the contribution of  $\varphi_n$  to the molecular wave function  $\Psi$  (eq. 12) is guaranteed according to:

$$c_n \varphi_n = c_{n_1} \varphi_{n_1} + c_{n_2} \varphi_{n_2}, \quad (26)$$

In order to limit the additional computational cost introduced by each cloning event, the number of cloning events should be restricted. This is done by introducing three cloning criteria.<sup>54</sup> The first criterion quantifies whether the electronic distribution for a given configuration is sufficiently spread over several excited states:

$$W_n = \frac{1}{\sum_I^N |a_I^{(n)}|^4} > \delta_1, \quad (27)$$

where  $W_n$  takes values between 1 and the number of excited states  $N$  considered. For  $W_n = 1$  only one of the excited states is populated, while for  $W_n = N$  the electronic population is evenly distributed among all the excited states considered. Following previous studies on combinations of PPE dendrimer building blocks like the one selected here as a representative example, a value of  $\delta_1 = 1.5$  was used.

The second criterion compares both the direction and magnitude of the weighted sum of gradients and the gradient of the state  $M$  with the highest population by means of the generalized angle:

$$\theta^{(n)} = \arccos \left( 2 \frac{\nabla_{\mathbf{R}} V_{\mathbf{M}}^{(n)} \cdot \sum_I |a_I^{(n)}|^2 \nabla_{\mathbf{R}} V_I^{(n)}}{|\nabla_{\mathbf{R}} V_{\mathbf{M}}^{(n)}|^2 + \left| \sum_I |a_I^{(n)}|^2 \nabla_{\mathbf{R}} V_I^{(n)} \right|^2} \right) > \delta_2, \quad (28)$$

where a value of  $\delta_2 = \frac{\pi}{18}$  was used in the simulations presented in this work.

Finally, the third criterion prevents the algorithm from cloning in the strong coupling regime. Otherwise, uncontrolled exponential growth of the basis set could occur in this region, leading to an inefficient sampling with several trajectories exploring the same configurational space:

$$\sum_I \left| 2 \frac{\Re \{ a_I^{(n)} (a_M^{(n)})^* \} \dot{\mathbf{R}} \cdot \mathbf{d}_{IM}}{|a_M^{(n)}|^2} \right| < \delta_3, \quad (29)$$

where  $\Re$  stands for the *real part*. A value of  $\delta_3 = 0.005$  was set for the simulations in this work. The selection of these combination of  $\delta_1$ ,  $\delta_2$ , and  $\delta_3$  has guaranteed a substantial amount of cloning events **for a diverse set of dendritic molecules as reported previously,<sup>88</sup> which** that allows to analyze the effects that the presence of different branching relaxation pathways have on the simulations without increasing the computational cost to prohibitive values.

### 2.3 Other essential features related to computational efficiency and vibrational analysis

Additional NEXMD features implemented in the original release of the software package and retained in the updated NEXMD **v2.0** release include useful tools for molecular dynamics simulations such as the Langevin thermostat,<sup>119</sup> geometry optimization routine, continuum solvation models,<sup>120,121</sup> trivial unavoided crossings<sup>113,122</sup> and decoherence corrections.<sup>112</sup> The package also incorporates practical analyses of electronic excitations in terms of orbital distribution of transition density and its time-dependent flux<sup>67,123</sup> as well as real-space representation of transition density matrices.<sup>96,124,125</sup> These features are discussed in detail elsewhere.<sup>50</sup> NEXMD **v2.0** incorporates additional new features besides the implementation of EHR and AIMC methods (see Table I).

NEXMD **v2.0** has been particularly developed to deal with photophysics of large conjugated molecules involving hundreds of atoms and large densities of states. Most of the initial excited states are ultrafast depopulated during the very firsts few femtoseconds after photoexcitation transferring their energy to intermediate states. In order to improve the computational efficiency, NEXMD **v2.0** includes an on-the-fly state limiting method to eliminate states that are no longer essential for the non-radiative relaxation dynamics during TSH dynamics.<sup>126</sup> A threshold of  $n$  states is used and all states above the current state  $\alpha + n$  are removed throughout the simulations.

The photophysics of large conjugated molecular systems involves electronic and vibrational energy relaxation and redistributions that frequently occurs concomitantly. These processes can involve one or a few vibronic relaxation pathways in which only a few vibrational degrees of freedom are active. In order to facilitate this vibrational analysis, NEXMD **v2.0** incorporates Hessian and normal-mode calculation,<sup>127</sup> that are computed numerically from finite

differences of the analytical ground- or excited-states gradients. Besides, the impact of specific vibrations can be evaluated by performing simulations by selectively freezing certain motions. NEXMD v2.0 incorporates the possibility to apply distance and normal modes constraints in the simulations. Distances constraints are implemented according to the Rattle algorithm,<sup>128</sup> and normal modes constraints are enabled by the FrozeNM algorithm.<sup>89</sup>

### 3. Exemplary simulations of photoinduced dynamics

The photoinduced dynamics of a PPE dendrimer building block has been simulated to illustrate the different NAMD methods implemented in NEXMD v2.0 using CIS/AM1 electronic structure description. **Technical details and parameters for these simulations can be found in the Supplementary Information.** The inset in **Figure 1** shows the geometry of the molecule and the orbital localization of the respective transition densities for the first three singlet excited states calculated at the ground state minimum energy geometry. While  $S_3$  is localized in the center of the dendrimer,  $S_2$  and  $S_1$  are Frenkel exciton-like states resulting from symmetric and antisymmetric superpositions of contributions from the individual side branches. The delocalization between equivalent branches is expected for symmetric configurations such as the ground state optimal geometry for PPE. Thermal structural fluctuations break the delocalization pronounced for the ground state structure and lead to localized exciton states. This initial analysis predicts the expected mechanism of electronic relaxation after the initial excitation to  $S_3$ : an electronic energy transfer from the center of the molecule to the branches, followed by coherent or incoherent vibrational oscillations between the branches. In order to describe this mechanism, nonadiabatic excited-state molecular dynamics were performed using TSH, EHR and AIMC methods. Simulations starting from the pure  $S_3$  state provide information about the relaxation process from the center of the molecule to the branches (these simulations are provided for a reference in Supplemental Information), while calculations starting from  $S_2$  reveal the coherent interplay between the branches as illustrated below.

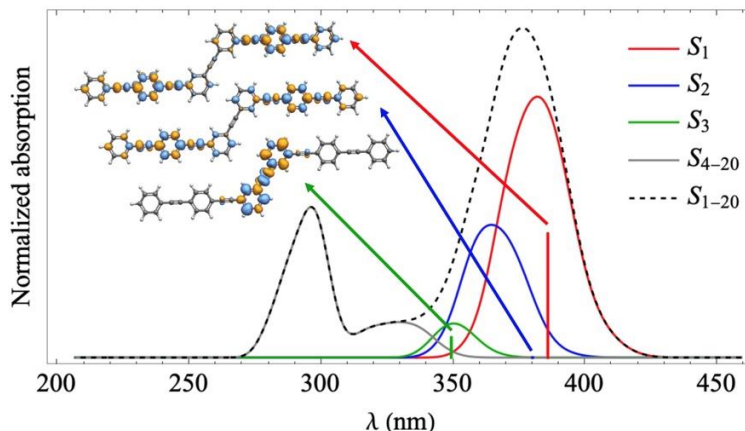


**Figure 1.** Normalized simulated absorption spectra of the PPE dendrimer building block with contributions from the first 20 excited states (black dashed line). Individual contributions from the first three excited states are shown as colored solid lines. Vertical lines show the corresponding energies and relative oscillator strengths for these three states at the minimum ground-state energy configuration. Arrows point to insets depicting the corresponding CIS electronic transition density localizations in real space.

**Figure 2** shows the evolution in time of the excited state populations for the first two excited states after an initial vertical excitation to the  $S_2$  state using TSH, EHR, and AIMC. The three methods show similar relaxation time scales. TSH leads to the fastest relaxation as was observed previously for many molecular systems.<sup>88</sup> While TSH electronic populations are calculated as the fraction of trajectories evolving on each state at any given time,<sup>129</sup> EHR and AIMC electronic populations are evaluated using the adiabatic population operator  $\langle \hat{P}_K \rangle$  (eq. 19) neglecting the nuclear overlap between different initial conditions. In the case of EHR simulations,  $\langle \hat{P}_K \rangle$  is simplified to the average values of  $|a_K^{(n)}|^2$ , and for AIMC it only includes clones originated from the same initial conditions. Note that TSH uses the instantaneous decoherence (ID) approach that resets the quantum amplitude of the current state to unity after every attempted hop (regardless of whether hops are allowed or forbidden).<sup>112</sup> EHR and AIMC lead to very similar dynamics showing slower relaxations, revealing a coherent oscillations in the population, which are not observed in TSH dynamics. This coherence is observed as an oscillatory interchange of electronic populations between  $S_1$  and  $S_2$  states during the first 20 fs of EHR and AIMC dynamics after photoexcitation. These oscillations reveal a coherent vibronic interplay that is missing in TSH dynamics. The lack of coherence in TSH is partially attributed to an instantaneous decoherence correction,<sup>15</sup> which assumes that the divergent wave packets become immediately decoupled. At the end of modeled excited-state dynamics, the  $S_1$  population obtained by AIMC dynamics is positioned in between TSH and EHR final values. The AIMC dynamics may be more physically relevant compared to the average Ehrenfest force, as discussed in the preceding section.

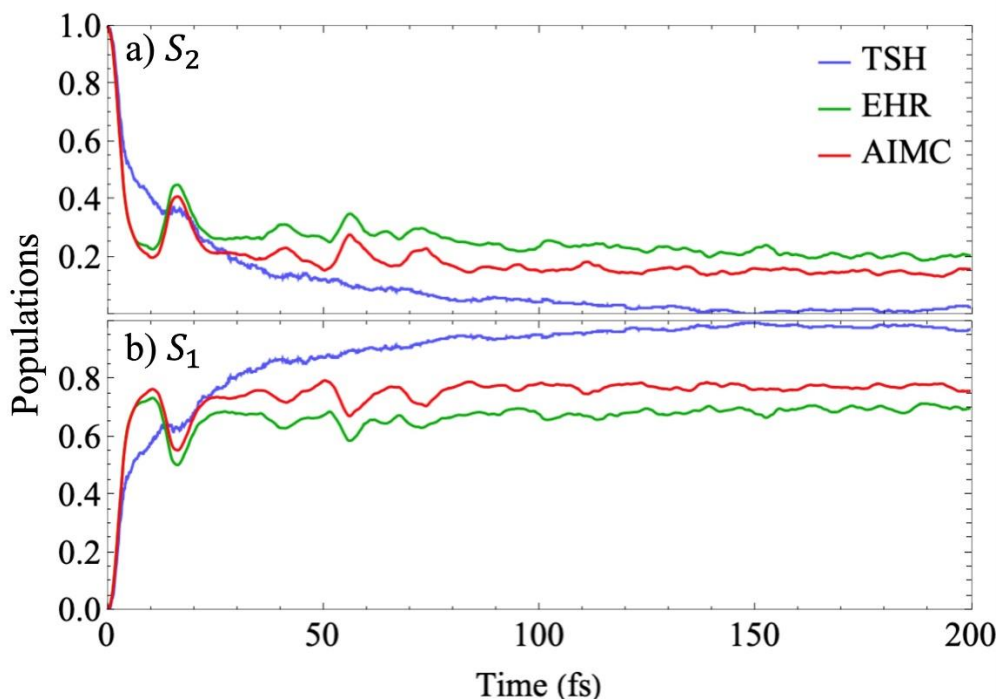


**Figure 2.** Evolution in time of the populations of a)  $S_2$  and b)  $S_1$  when the system is excited initially at  $S_2$  for different nonadiabatic molecular dynamics methods.

The evolution in time of  $\langle \hat{\rho}_X \rangle$  (eq. 20), i.e., the fraction of transition density localized in the two 3-ring fragments is shown in **Figure 3**. As shown in the inset, the two 3-ring fragments are assigned as “higher” (H) and “lower” (L) according to their correspondingly higher or lower values of  $\langle \hat{\rho}_X \rangle$  at  $t = 0$  for each initial condition. Thermal fluctuations initially localize the states that otherwise should be delocalized by symmetry, as it is shown in **Figure 1** for the ground-state geometry. The results obtained during TSH, EHR and AIMC dynamics simulations are similar qualitatively, with a faster energy redistribution between the 3-ring linear fragments observed during TSH dynamics compared to EHR and AIMC. We observe an equivalent distribution of  $\langle \hat{\rho}_X \rangle$  between the 3-ring linear fragments toward the end of the simulation due to the thermally induced reorganization of the exciton over the equivalent fragments, irrespective of its initial localization.<sup>16</sup> Further analysis of individual trajectories indicates that this final distribution of  $\langle \hat{\rho}_X \rangle$  between the two fragments is attributed to a localization of the exciton on either fragment with H and L having equal probability across the ensemble rather than to a uniform delocalization over the entire dendrimer. Overall, the evolution in time of  $\langle \hat{\rho}_X \rangle$  is in line with results displayed in **Figure 2**. That is, TSH dynamics show very fast damping of the oscillations, while for EHR and AIMC dynamics, oscillations persist for more than 100 fs after photoexcitation. These oscillations are damped slightly faster for AIMC due to the natural decoherence introduced by the bifurcations of the wave packet in the algorithm, as reported previously.<sup>88</sup>

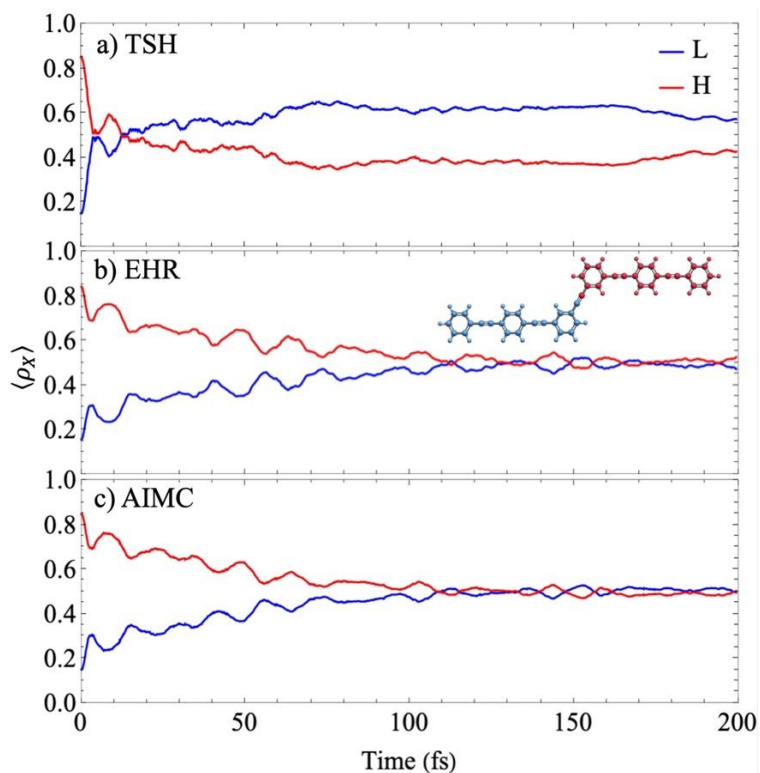


**Figure 3.** Evolution in time of  $\langle \hat{\rho}_X \rangle$ , i.e., the fraction of transition density localized over different fragments  $X$  of the molecule during a) TSH, b) EHR and c) AIMC dynamics after photoexcitation to  $S_2$ . The spatial descriptor assigns as “higher” (H) or “lower” (L) the 3-ring linear fragments with higher and lower transition density at  $t = 0$ , respectively. The inset in b) depicts the molecule delineation into fragments.

The use of the “on the fly” state limiting method can significantly decrease the computational expense in trajectory surface hopping simulations of realistically large molecular systems with a dense manifold of excited states participating in the dynamics.<sup>126</sup> In order to exemplify this approach, we photoexcite the PPE dendrimer building block at the  $S_{20}$  state. The use of the on-the-fly state limiting method increases the computational efficiency up to 5 times. This is achieved by the fast reduction in the number states during simulations (see **Figure 4(a, b)**).

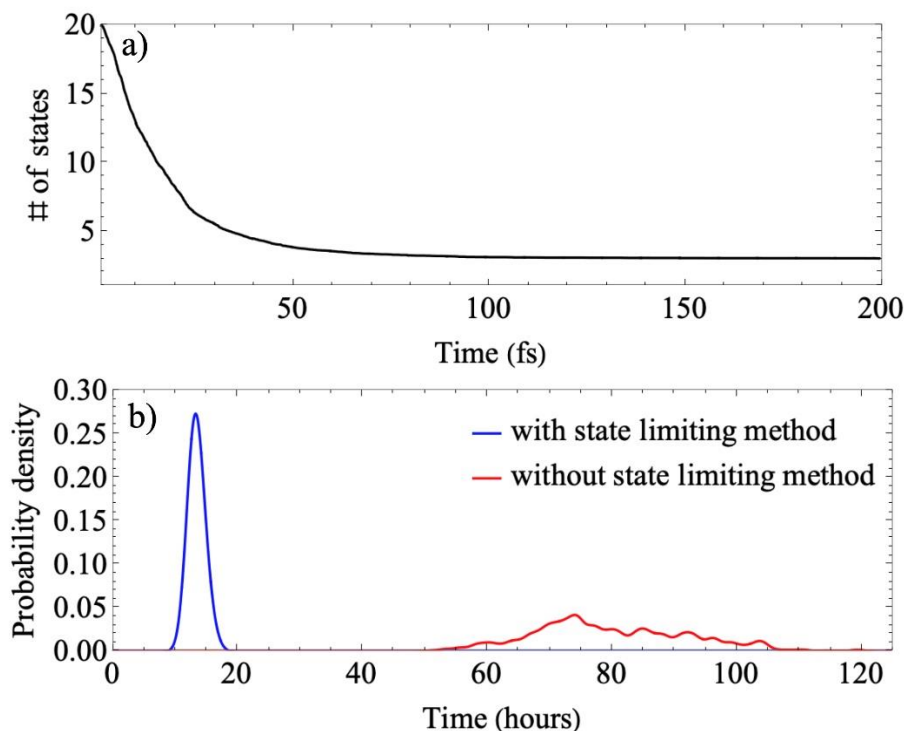


**Figure 4.** (a) Evolution in time of the # of states applying the on-the-fly state limiting method to eliminate states that are no longer essential for the non-radiative relaxation dynamics during TSH simulations; (b) Comparison of the distribution of computational time required for simulations with and without applying the on-the-fly state limiting method. A threshold of 2 states is used and all states above the current state  $\alpha + 2$  are removed throughout the simulations.

NEXMD v2.0 allows to analyze the impact of specific nuclear motions by performing TSH non-adiabatic excited state molecular dynamics in the presence of constraints on certain distances or vibrational normal modes. In order to illustrate this feature, simulations constraining the four triple bonds localized in the 3-ring linear units in a PPE dendrimer building block, have been performed. **Figure 5** shows that these constrains do not have a significant impact in the electronic relaxation. Nevertheless, a more efficient slowdown of the electronic relaxation can be achieved by performing normal-modes constraints. **Figure 5** shows the results of introducing constraints into the two normal modes that overlap the most with the direction of  $S_2 \rightarrow S_1$  transition, dictated by the nonadiabatic coupling vector  $\mathbf{d}_{12}$ . Despite that these normal modes involve concerted motions of stretching in the direction of the triple bonds, they also imply minor motions associated to the highest frequency vibrational normal modes of phenyl rings. This result reveals the main role of these selective vibrational motions on the energy transfer process and can be a useful guide for the development of reduced dimensionality Hamiltonians.

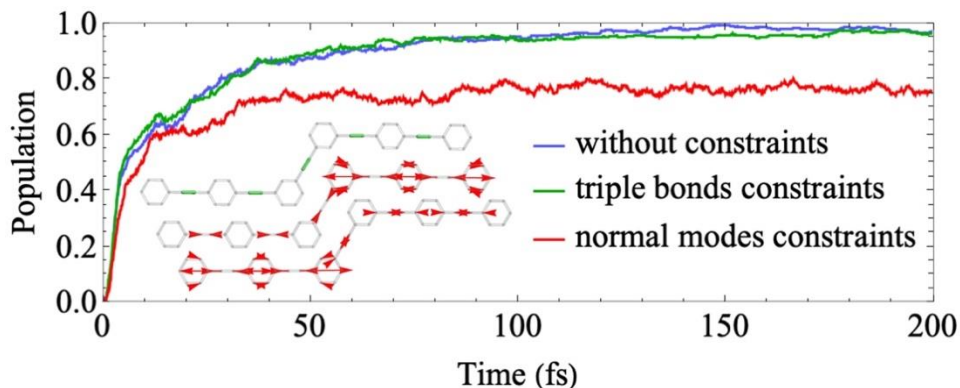


**Figure 5.** Evolution in time of the average population of  $S_1$  electronic state without constraints, with constraints applied to the four triple bonds localized on the 3-ring linear units, and with normal mode constraints applied to the two normal modes that overlap the most with the nonadiabatic coupling vector. The inset show the triple bonds localizations (green) and the two normal modes (red).

## 4. Conclusions

The second release of the NEXMD (Nonadiabatic EXcited state Molecular Dynamics) software package incorporates Ehrenfest (EHR) hybrid quantum-classical dynamics and the Ab-Initio Multiple Cloning (AIMC) sampling technique for Multiconfigurational Ehrenfest quantum dynamics method, complementing the previously implemented trajectory surface hopping (TSH) method. Besides, other significant features are summarized in Table I. NEXMD v2.0 expands the range of applications to a larger variety of photophysical processes in multichromophore organic molecules. In particular, the AIMC non-adiabatic molecular dynamics algorithm is a controlled approximation allowing for an appropriate description of electron-vibrational coherences appearing in many molecular systems. The implementation of TSH, EHR, and AIMC on the same footing within the updated NEXMD v2.0 framework permits users to explore individual algorithms and directly compare different methods applied to a particular molecular system or a process of interest. Further, additional NEXMD v2.0 capabilities such as extensive analysis of vibrational degrees of freedom and ability to artificially exclude structural degrees of freedom of choice from non-adiabatic dynamics, provide practical tools for designing flexible numerical experiments. The presented illustrative examples demonstrate some of the weaknesses and strengths of these NAMD methods for the case of a PPE dendrimer. While both TSH and EHR dynamics may not properly treat decoherence in the electronic systems, AIMC describes decoherences in a natural way. Therefore, the AIMC method is suitable for practical applications, like time-dependent nonlinear spectroscopic signals conditioned by the presence of vibronic coherences. Broader application with NEXMD v2.0 can thus validate various non-adiabatic algorithms and stimulate further method development towards more accurate description of photophysical processes in multichromophore organic molecules.

Altogether, the NEXMD v2.0 software represents a numerically efficient method to perform excited state dynamics on molecules and molecular clusters. Perhaps the largest weakness of the current method is in the underlying semi-empirical Hamiltonians underpinning the numerical efficiency but allowing only a semi quantitative accuracy. Here we mention that most of the NEXMD features and algorithms have been recently implemented into NWChem software

package<sup>42</sup> allowing interfacing more accurate but numerically expensive time-dependent Density Functional Theory description of electronically excited states. Further, recent advances into interfacing machine learning techniques with semi-empirical quantum mechanics<sup>130–133</sup> promise to provide a breakthrough in semi-empirical accuracy. Additionally, the development of SIMD (Same Instruction, Multiple Data) architectures provides an avenue for significantly decreasing the computational challenges associated with simulations involving many distinct trajectories. Future code additions such as periodic boundary conditions will open possibilities toward modeling solids. Besides, future implementations of nonlinear spectroscopic signals calculations from dynamical information, like transient absorption, 2D electronic spectroscopy and X-Ray nonlinear probes<sup>14,16</sup> will provide a more direct comparison with experiments. These additional capabilities promise to provide significant advances in the modeling of photocatalyzed reactions, light absorption, and reactive chemistry critical to a green energy future.

## Acknowledgements

S.T. acknowledges support from the U.S. DOE, Office of Science, Office of Basic Energy Sciences under Triad National Security, LLC (“Triad”) contract grant # 89233218CNA000001 (FWP: LANLE3T1). This work was performed in part at the Center for Integrated Nanotechnology (CINT) at Los Alamos National Laboratory (LANL), a U.S. DOE and Office of Basic Energy Sciences user facility. This research used resources provided by the LANL Institutional Computing Program. Y.Z. acknowledges the support from the Laboratory Directed Research and Development (LDRD) program of LANL. S.F.-A. and H. N.-Y. acknowledge the support of CONICET, UNQ, and ANPCyT (PICT 2018-02360). The work was supported by the Chemical Sciences, Geosciences, and Biosciences division, Office of Basic Energy Sciences, Office of Science, U.S. DOE through Award DE-SC0022225. S.M. also acknowledges the Hagler Institute for Advanced Study at Texas A&M University, from which he is a fellow. L. N. M. and S. S. acknowledge the support from the National Science Foundation (NSF) under grant no. DMR-1847774, and through the Center for Complex and Active Materials at the University of California, Irvine (DMR-2011967).

**Supporting Information** contains computational and technical details for the exemplary simulations and a comparison between non-adiabatic excited state methods when exciting to  $S_3$ .

## Notes

The authors declare no competing financial interest.  
Program code, license, and documentation may be accessed at:  
<https://github.com/lanl/NEXMD>.

## References

- (1) Polli, D.; Altoè, P.; Weingart, O.; Spillane, K. M.; Manzoni, C.; Brida, D.; Tomasello, G.; Orlandi, G.; Kukura, P.; Mathies, R. A.; Garavelli, M.; Cerullo, G. Conical Intersection Dynamics of the Primary Photoisomerization Event in Vision. *Nature* **2010** *467*:7314 **2010**, *467* (7314), 440–443. <https://doi.org/10.1038/nature09346>.

- (2) Bricker, W. P.; Shenai, P. M.; Ghosh, A.; Liu, Z.; Enriquez, M. G. M.; Lambrev, P. H.; Tan, H.-S.; Lo, C. S.; Tretiak, S.; Fernandez-Alberti, S.; Zhao, Y. Non-Radiative Relaxation of Photoexcited Chlorophylls: Theoretical and Experimental Study. *Sci Rep* **2015**, *5* (1), 13625. <https://doi.org/10.1038/srep13625>.
- (3) Shenai, P. M.; Fernandez-Alberti, S.; Bricker, W. P.; Tretiak, S.; Zhao, Y. Internal Conversion and Vibrational Energy Redistribution in Chlorophyll A. *J Phys Chem B* **2016**, *120* (1), 49–58. <https://doi.org/10.1021/acs.jpcc.5b09548>.
- (4) Scholes, G. D.; Fleming, G. R.; Chen, L. X.; Aspuru-Guzik, A.; Buchleitner, A.; Coker, D. F.; Engel, G. S.; van Grondelle, R.; Ishizaki, A.; Jonas, D. M.; Lundeen, J. S.; McCusker, J. K.; Mukamel, S.; Ogilvie, J. P.; Olaya-Castro, A.; Ratner, M. A.; Spano, F. C.; Whaley, K. B.; Zhu, X. Using Coherence to Enhance Function in Chemical and Biophysical Systems. *Nature* **2017**, *543* (7647), 647–656. <https://doi.org/10.1038/nature21425>.
- (5) Granström, M.; Petritsch, K.; Arias, A. C.; Lux, A.; Andersson, M. R.; Friend, R. H. Laminated Fabrication of Polymeric Photovoltaic Diodes. *Nature* **1998**, *395* (6699), 257–260. <https://doi.org/10.1038/26183>.
- (6) Cao, Y.; Parker, I. D.; Yu, G.; Zhang, C.; Heeger, A. J. Improved Quantum Efficiency for Electroluminescence in Semiconducting Polymers. *Nature* **1999**, *397*:6718 **1999**, *397* (6718), 414–417. <https://doi.org/10.1038/17087>.
- (7) Tretiak, S.; Saxena, A.; Martin, R. L.; Bishop, A. R. Conformational Dynamics of Photoexcited Conjugated Molecules. *Phys Rev Lett* **2002**, *89* (9), 097402. <https://doi.org/10.1103/PhysRevLett.89.097402>.
- (8) Kasha, M. Characterization of Electronic Transitions in Complex Molecules. *Discuss Faraday Soc* **1950**, *9*, 14. <https://doi.org/10.1039/df9500900014>.
- (9) Robb, M. A.; Garavelli, M.; Olivucci, M.; Bernardi, F. A Computational Strategy for Organic Photochemistry; 2007; pp 87–146. <https://doi.org/10.1002/9780470125922.ch2>.
- (10) Jiang, Y.; McNeill, J. Light-Harvesting and Amplified Energy Transfer in Conjugated Polymer Nanoparticles. *Chem Rev* **2017**, *117* (2), 838–859. <https://doi.org/10.1021/acs.chemrev.6b00419>.
- (11) Huix-Rotllant, M.; Tamura, H.; Burghardt, I. Concurrent Effects of Delocalization and Internal Conversion Tune Charge Separation at Regioregular Polythiophene-Fullerene Heterojunctions. *Journal of Physical Chemistry Letters* **2015**, *6* (9), 1702–1708. [https://doi.org/10.1021/ACS.JPCLETT.5B00336/SUPPL\\_FILE/JZ5B00336\\_SI\\_002.PDF](https://doi.org/10.1021/ACS.JPCLETT.5B00336/SUPPL_FILE/JZ5B00336_SI_002.PDF).
- (12) Brédas, J.-L. L.; Beljonne, D.; Coropceanu, V.; Cornil, J. J. Charge-Transfer and Energy-Transfer Processes in  $\pi$ -Conjugated Oligomers and Polymers: A Molecular Picture. *Chem Rev* **2004**, *104* (11), 4971–5004. <https://doi.org/10.1021/cr040084k>.
- (13) Adamska, L.; Nayyar, I.; Chen, H.; Swan, A. K.; Oldani, N.; Fernandez-Alberti, S.; Golder, M. R.; Jasti, R.; Doorn, S. K.; Tretiak, S. Self-Trapping of Excitons, Violation of Condon Approximation, and Efficient Fluorescence in Conjugated Cycloparaphenylenes. *Nano Lett* **2014**, *14* (11), 6539–6546. <https://doi.org/10.1021/nl503133e>.
- (14) Keefer, D.; Freixas, V. M.; Song, H.; Tretiak, S.; Fernandez-Alberti, S.; Mukamel, S. Monitoring Molecular Vibronic Coherences in a Bichromophoric Molecule by Ultrafast X-Ray Spectroscopy. *Chem Sci* **2021**, *12* (14), 5286–5294. <https://doi.org/10.1039/D0SC06328B>.

- (15) Freixas, V. M.; Tretiak, S.; Makhov, D. V.; Shalashilin, D. V.; Fernandez-Alberti, S. Vibronic Quantum Beating between Electronic Excited States in a Heterodimer. *J Phys Chem B* **2020**, *124* (19), 3992–4001. <https://doi.org/10.1021/acs.jpcc.0c01685>.
- (16) Freixas, V. M.; Keefer, D.; Tretiak, S.; Fernandez-Alberti, S.; Mukamel, S. Ultrafast Coherent Photoexcited Dynamics in a Trimeric Dendrimer Probed by X-Ray Stimulated-Raman Signals. *Chem Sci* **2022**, *13* (21), 6373–6384. <https://doi.org/10.1039/D2SC00601D>.
- (17) Salehi, A.; Fu, X.; Shin, D. H.; So, F. Recent Advances in OLED Optical Design. *Advanced Functional Materials*. Wiley-VCH Verlag April 11, 2019, p 1808803. <https://doi.org/10.1002/adfm.201808803>.
- (18) Wang, N.; Tong, X.; Burlingame, Q.; Yu, J.; Forrest, S. R. Photodegradation of Small-Molecule Organic Photovoltaics. *Solar Energy Materials and Solar Cells* **2014**, *125*, 170–175. <https://doi.org/10.1016/j.solmat.2014.03.005>.
- (19) Wolfer, P.; Armin, A.; Pivrikas, A.; Velusamy, M.; Burn, P. L.; Meredith, P. Solution Structure: Defining Polymer Film Morphology and Optoelectronic Device Performance. *J Mater Chem C Mater* **2014**, *2* (1), 71–77. <https://doi.org/10.1039/c3tc31812e>.
- (20) Zhugayevych, A.; Tretiak, S. Theoretical Description of Structural and Electronic Properties of Organic Photovoltaic Materials. <http://dx.doi.org/10.1146/annurev-physchem-040214-121440> **2015**, *66*, 305–330. <https://doi.org/10.1146/ANNUREV-PHYSCHEM-040214-121440>.
- (21) Sirringhaus, H.; Kawase, T.; Friend, R. H.; Shimoda, T.; Inbasekaran, M.; Wu, W.; Woo, E. P. High-Resolution Inkjet Printing of All-Polymer Transistor Circuits. *Science (1979)* **2000**, *290* (5499), 2123–2126. <https://doi.org/10.1126/SCIENCE.290.5499.2123>.
- (22) Lee, K. E.; Lee, J. U.; Seong, D. G.; Um, M.-K.; Lee, W. Highly Sensitive Ultraviolet Light Sensor Based on Photoactive Organic Gate Dielectrics with an Azobenzene Derivative. *Journal of Physical Chemistry C* **2016**, *120* (40), 23172–23179. <https://doi.org/10.1021/ACS.JPCC.6B08427>.
- (23) Satishkumar, B. C.; Brown, L. O.; Gao, Y.; Wang, C.-C.; Wang, H.-L.; Doorn, S. K. Reversible Fluorescence Quenching in Carbon Nanotubes for Biomolecular Sensing. *Nature Nanotechnology* **2007**, *2* (9), 560–564. <https://doi.org/10.1038/nnano.2007.261>.
- (24) Maksimov, E. G.; Yaroshevich, I. A.; Tsoraev, G. V.; Sluchanko, N. N.; Slutskaya, E. A.; Shamborant, O. G.; Bobik, T. V.; Friedrich, T.; Stepanov, A. V. A Genetically Encoded Fluorescent Temperature Sensor Derived from the Photoactive Orange Carotenoid Protein. *Scientific Reports* **2019**, *9* (1), 1–9. <https://doi.org/10.1038/s41598-019-45421-7>.
- (25) Li, H.; Wang, J.; Wang, X.; Lin, H.; Li, F. Perylene-Based Photoactive Material as a Double-Stranded DNA Intercalating Probe for Ultrasensitive Photoelectrochemical Biosensing. *ACS Appl Mater Interfaces* **2019**, *11* (18), 16958–16964. <https://doi.org/10.1021/ACSAMI.9B04299>.
- (26) Wilson, A.; Punginelli, C.; Gall, A.; Bonetti, C.; Alexandre, M.; Routaboul, J.-M.; Kerfeld, C. A.; Grondelle, R. van; Robert, B.; Kennis, J. T. M.; Kirilovsky, D. A Photoactive Carotenoid Protein Acting as Light Intensity Sensor. *Proceedings of the National Academy of Sciences* **2008**, *105* (33), 12075–12080. <https://doi.org/10.1073/PNAS.0804636105>.

- (27) Singer, N. K.; Sánchez-Murcia, P. A.; Ernst, M.; González, L. Unravelling the Turn-On Fluorescence Mechanism of a Fluorescein-Based Probe in GABAA Receptors. *Angewandte Chemie International Edition* **2022**, *61* (30), e202205198. <https://doi.org/10.1002/ANIE.202205198>.
- (28) Romero, N. A.; Nicewicz, D. A. Organic Photoredox Catalysis. *Chem Rev* **2016**, *116* (17), 10075–10166. [https://doi.org/10.1021/ACS.CHEMREV.6B00057/ASSET/IMAGES/MEDIUM/CR-2016-00057Y\\_0192.GIF](https://doi.org/10.1021/ACS.CHEMREV.6B00057/ASSET/IMAGES/MEDIUM/CR-2016-00057Y_0192.GIF).
- (29) Brédas, J. L.; Norton, J. E.; Cornil, J.; Coropceanu, V. Molecular Understanding of Organic Solar Cells: The Challenges. *Acc Chem Res* **2009**, *42* (11), 1691–1699. <https://doi.org/10.1021/ar900099h>.
- (30) Schmidt-Hansberg, B.; Sanyal, M.; Klein, M. F. G.; Pfaff, M.; Schnabel, N.; Jaiser, S.; Vorobiev, A.; Müller, E.; Colsmann, A.; Scharfer, P.; Gerthsen, D.; Lemmer, U.; Barrena, E.; Schabel, W. Moving through the Phase Diagram: Morphology Formation in Solution Cast Polymer-Fullerene Blend Films for Organic Solar Cells. *ACS Nano* **2011**, *5* (11), 8579–8590. <https://doi.org/10.1021/nn2036279>.
- (31) Shao, Y.; Gan, Z.; Epifanovsky, E.; Gilbert, A. T. B.; Wormit, M.; Kussmann, J.; Lange, A. W.; Behn, A.; Deng, J.; Feng, X.; Ghosh, D.; Goldey, M.; Horn, P. R.; Jacobson, L. D.; Kaliman, I.; Khaliullin, R. Z.; Kuš, T.; Landau, A.; Liu, J.; Proynov, E. I.; Rhee, Y. M.; Richard, R. M.; Rohrdanz, M. A.; Steele, R. P.; Sundstrom, E. J.; Woodcock, H. L.; Zimmerman, P. M.; Zuev, D.; Albrecht, B.; Alguire, E.; Austin, B.; Beran, G. J. O.; Bernard, Y. A.; Berquist, E.; Brandhorst, K.; Bravaya, K. B.; Brown, S. T.; Casanova, D.; Chang, C. M.; Chen, Y.; Chien, S. H.; Closser, K. D.; Crittenden, D. L.; Diedenhofen, M.; Distasio, R. A.; Do, H.; Dutoi, A. D.; Edgar, R. G.; Fatehi, S.; Fusti-Molnar, L.; Ghysels, A.; Golubeva-Zadorozhnaya, A.; Gomes, J.; Hanson-Heine, M. W. D.; Harbach, P. H. P.; Hauser, A. W.; Hohenstein, E. G.; Holden, Z. C.; Jagau, T. C.; Ji, H.; Kaduk, B.; Khistyayev, K.; Kim, J.; Kim, J.; King, R. A.; Klunzinger, P.; Kosenkov, D.; Kowalczyk, T.; Krauter, C. M.; Lao, K. U.; Laurent, A. D.; Lawler, K. V.; Levchenko, S. V.; Lin, C. Y.; Liu, F.; Livshits, E.; Lochan, R. C.; Luenser, A.; Manohar, P.; Manzer, S. F.; Mao, S. P.; Mardirossian, N.; Marenich, A. V.; Maurer, S. A.; Mayhall, N. J.; Neuscamman, E.; Oana, C. M.; Olivares-Amaya, R.; Oneill, D. P.; Parkhill, J. A.; Perrine, T. M.; Peverati, R.; Prociuk, A.; Rehn, D. R.; Rosta, E.; Russ, N. J.; Sharada, S. M.; Sharma, S.; Small, D. W.; Sodt, A.; Stein, T.; Stück, D.; Su, Y. C.; Thom, A. J. W.; Tsuchimochi, T.; Vanovschi, V.; Vogt, L.; Vydrov, O.; Wang, T.; Watson, M. A.; Wenzel, J.; White, A.; Williams, C. F.; Yang, J.; Yeganeh, S.; Yost, S. R.; You, Z. Q.; Zhang, I. Y.; Zhang, X.; Zhao, Y.; Brooks, B. R.; Chan, G. K. L.; Chipman, D. M.; Cramer, C. J.; Goddard, W. A.; Gordon, M. S.; Hehre, W. J.; Klamt, A.; Schaefer, H. F.; Schmidt, M. W.; Sherrill, C. D.; Truhlar, D. G.; Warshel, A.; Xu, X.; Aspuru-Guzik, A.; Baer, R.; Bell, A. T.; Besley, N. A.; Chai, J. Da; Dreuw, A.; Dunietz, B. D.; Furlani, T. R.; Gwaltney, S. R.; Hsu, C. P.; Jung, Y.; Kong, J.; Lambrecht, D. S.; Liang, W.; Ochsenfeld, C.; Rassolov, V. A.; Slipchenko, L. V.; Subotnik, J. E.; Van Voorhis, T.; Herbert, J. M.; Krylov, A. I.; Gill, P. M. W.; Head-Gordon, M. Advances in Molecular Quantum Chemistry Contained in the Q-Chem 4 Program Package. <https://doi.org/10.1080/00268976.2014.952696> **2014**, *113* (2), 184–215. <https://doi.org/10.1080/00268976.2014.952696>.

- (32) Richter, M.; Marquetand, P.; González-Vázquez, J.; Sola, I.; González, L. SHARC: Ab Initio Molecular Dynamics with Surface Hopping in the Adiabatic Representation Including Arbitrary Couplings. *J Chem Theory Comput* **2011**, *7* (5), 1253–1258. <https://doi.org/10.1021/ct1007394>.
- (33) Avagliano, D.; Bonfanti, M.; Garavelli, M.; González, L. QM/MM Nonadiabatic Dynamics: The SHARC/COBRAMM Approach. *J Chem Theory Comput* **2021**, *17* (8), 4639–4647. <https://doi.org/10.1021/acs.jctc.1c00318>.
- (34) Mai, S.; Marquetand, P.; González, L. Nonadiabatic Dynamics: The SHARC Approach. *Wiley Interdiscip Rev Comput Mol Sci* **2018**, *8* (6). <https://doi.org/10.1002/WCMS.1370>.
- (35) Weingart, O.; Nenov, A.; Altoè, P.; Rivalta, I.; Segarra-Martí, J.; Dokukina, I.; Garavelli, M. COBRAMM 2.0 — A Software Interface for Tailoring Molecular Electronic Structure Calculations and Running Nanoscale (QM/MM) Simulations. *Journal of Molecular Modeling* **2018**, *24* (9), 1–30. <https://doi.org/10.1007/S00894-018-3769-6>.
- (36) Barbatti, M.; Ruckebauer, M.; Plasser, F.; Pittner, J.; Granucci, G.; Persico, M.; Lischka, H. Newton-X: A Surface-Hopping Program for Nonadiabatic Molecular Dynamics. *Wiley Interdiscip Rev Comput Mol Sci* **2014**, *4* (1), 26–33. <https://doi.org/10.1002/WCMS.1158>.
- (37) Barbatti, M.; Granucci, G.; Persico, M.; Ruckebauer, M.; Vazdar, M.; Eckert-Maksić, M.; Lischka, H. The On-the-Fly Surface-Hopping Program System Newton-X: Application to Ab Initio Simulation of the Nonadiabatic Photodynamics of Benchmark Systems. *J Photochem Photobiol A Chem* **2007**, *190* (2–3), 228–240. <https://doi.org/10.1016/j.jphotochem.2006.12.008>.
- (38) Akimov, A. V.; Prezhdo, O. V. The PYXAID Program for Non-Adiabatic Molecular Dynamics in Condensed Matter Systems. *J Chem Theory Comput* **2013**, *9* (11), 4959–4972. <https://doi.org/10.1021/ct400641n>.
- (39) Akimov, A. V.; Prezhdo, O. V. Advanced Capabilities of the PYXAID Program: Integration Schemes, Decoherence Effects, Multiexcitonic States, and Field-Matter Interaction. *J Chem Theory Comput* **2014**, *10* (2), 789–804. <https://doi.org/10.1021/ct400934c>.
- (40) Valiev, M.; Bylaska, E. J.; Govind, N.; Kowalski, K.; Straatsma, T. P.; Van Dam, H. J. J.; Wang, D.; Nieplocha, J.; Apra, E.; Windus, T. L.; De Jong, W. A. NWChem: A Comprehensive and Scalable Open-Source Solution for Large Scale Molecular Simulations. *Comput Phys Commun* **2010**, *181* (9), 1477–1489. <https://doi.org/10.1016/J.CPC.2010.04.018>.
- (41) Song, H.; Fischer, S. A.; Zhang, Y.; Cramer, C. J.; Mukamel, S.; Govind, N.; Tretiak, S. First Principles Nonadiabatic Excited-State Molecular Dynamics in NWChem. *J Chem Theory Comput* **2020**, *16* (10), 6418–6427. [https://doi.org/10.1021/ACS.JCTC.0C00295/SUPPL\\_FILE/CTOC00295\\_SI\\_001.PDF](https://doi.org/10.1021/ACS.JCTC.0C00295/SUPPL_FILE/CTOC00295_SI_001.PDF).
- (42) Song, H.; Freixas, V. M.; Fernandez-Alberti, S.; White, A. J.; Zhang, Y.; Mukamel, S.; Govind, N.; Tretiak, S. An Ab Initio Multiple Cloning Method for Non-Adiabatic Excited-State Molecular Dynamics in NWChem. *J Chem Theory Comput* **2021**, *17* (6), 3629–3643. [https://doi.org/10.1021/ACS.JCTC.1C00131/SUPPL\\_FILE/CT1C00131\\_SI\\_001.PDF](https://doi.org/10.1021/ACS.JCTC.1C00131/SUPPL_FILE/CT1C00131_SI_001.PDF).
- (43) Furche, F.; Ahlrichs, R.; Hättig, C.; Klopper, W.; Sierka, M.; Weigend, F. Turbomole. *WIREs Computational Molecular Science* **2014**, *4* (2), 91–100. <https://doi.org/10.1002/wcms.1162>.

- (44) Balasubramani, S. G.; Chen, G. P.; Coriani, S.; Diedenhofen, M.; Frank, M. S.; Franzke, Y. J.; Furche, F.; Grotjahn, R.; Harding, M. E.; Hättig, C.; Hellweg, A.; Helmich-Paris, B.; Holzer, C.; Huniar, U.; Kaupp, M.; Marefat Khah, A.; Karbalaee Khani, S.; Müller, T.; Mack, F.; Nguyen, B. D.; Parker, S. M.; Perlt, E.; Rappoport, D.; Reiter, K.; Roy, S.; Rückert, M.; Schmitz, G.; Sierka, M.; Tapavicza, E.; Tew, D. P.; van Wüllen, C.; Voora, V. K.; Weigend, F.; Wodyński, A.; Yu, J. M. TURBOMOLE: Modular Program Suite for Ab Initio Quantum-Chemical and Condensed-Matter Simulations. *J Chem Phys* **2020**, *152* (18), 184107. <https://doi.org/10.1063/5.0004635>.
- (45) Shakiba, M.; Smith, B.; Li, W.; Dutra, M.; Jain, A.; Sun, X.; Garashchuk, S.; Akimov, A. Libra: A Modular Software Library for Quantum Nonadiabatic Dynamics. *Software Impacts* **2022**, *14*, 100445. <https://doi.org/10.1016/j.simpa.2022.100445>.
- (46) Lee, I. S.; Ha, J.; Han, D.; Kim, T. I.; Moon, S. W.; Min, S. K. PyUNIxMD: A Python-based Excited State Molecular Dynamics Package. *J Comput Chem* **2021**, *42* (24), 1755–1766. <https://doi.org/10.1002/jcc.26711>.
- (47) Rego, L. G.; Oliboni, R. S.; Hoff, D. A.; Torres, A. DynEMol: Tools for Studying Dynamics of Electrons in Molecules. 2014. <https://sourceforge.net/projects/charge-transfer/> (accessed 2023-07-06).
- (48) Du, L.; Lan, Z. An On-the-Fly Surface-Hopping Program JADE for Nonadiabatic Molecular Dynamics of Polyatomic Systems: Implementation and Applications. *J Chem Theory Comput* **2015**, *11* (4), 1360–1374. <https://doi.org/10.1021/ct501106d>.
- (49) Zheng, Q.; Chu, W.; Zhao, C.; Zhang, L.; Guo, H.; Wang, Y.; Jiang, X.; Zhao, J. Ab Initio Nonadiabatic Molecular Dynamics Investigations on the Excited Carriers in Condensed Matter Systems. *WIREs Computational Molecular Science* **2019**, *9* (6). <https://doi.org/10.1002/wcms.1411>.
- (50) Malone, W.; Nebgen, B.; White, A.; Zhang, Y.; Song, H.; Bjorgaard, J. A.; Sifain, A. E.; Rodriguez-Hernandez, B.; Freixas, V. M.; Fernandez-Alberti, S.; Roitberg, A. E.; Nelson, T. R.; Tretiak, S. NEXMD Software Package for Nonadiabatic Excited State Molecular Dynamics Simulations. *J Chem Theory Comput* **2020**, *16* (9), 5771–5783. <https://doi.org/10.1021/acs.jctc.0c00248>.
- (51) Nelson, T. R.; White, A. J.; Bjorgaard, J. A.; Sifain, A. E.; Zhang, Y.; Nebgen, B.; Fernandez-Alberti, S.; Mozyrsky, D.; Roitberg, A. E.; Tretiak, S. Non-Adiabatic Excited-State Molecular Dynamics: Theory and Applications for Modeling Photophysics in Extended Molecular Materials. *Chem Rev* **2020**, *120* (4), 2215–2287. <https://doi.org/10.1021/acs.chemrev.9b00447>.
- (52) Tully, J. C.; Preston, R. K. Trajectory Surface Hopping Approach to Nonadiabatic Molecular Collisions: The Reaction of H + with D<sub>2</sub>. *J Chem Phys* **1971**, *55* (2), 562–572. <https://doi.org/10.1063/1.1675788>.
- (53) Fernandez-Alberti, S.; Makhov, D. V.; Tretiak, S.; Shalashilin, D. V. Non-Adiabatic Excited State Molecular Dynamics of Phenylene Ethynylene Dendrimer Using a Multiconfigurational Ehrenfest Approach. *Physical Chemistry Chemical Physics* **2016**, *18* (15), 10028–10040. <https://doi.org/10.1039/C5CP07332D>.
- (54) Freixas, V. M.; Fernandez-Alberti, S.; Makhov, D. V.; Tretiak, S.; Shalashilin, D. An Ab Initio Multiple Cloning Approach for the Simulation of Photoinduced Dynamics in Conjugated

- Molecules. *Physical Chemistry Chemical Physics* **2018**, *20* (26), 17762–17772. <https://doi.org/10.1039/C8CP02321B>.
- (55) Makhov, D. V.; Symonds, C.; Fernandez-Alberti, S.; Shalashilin, D. V. A b Initio Quantum Direct Dynamics Simulations of Ultrafast Photochemistry with Multiconfigurational Ehrenfest Approach. *Chem Phys* **2017**, *493*, 200–218. <https://doi.org/10.1016/j.chemphys.2017.04.003>.
- (56) Thouless, D. J. *The Quantum Mechanics of Many-Body Systems*; Academic Press, New York, 1972.
- (57) Jorgensen, P. Molecular and Atomic Applications of Time-Dependent Hartree-Fock Theory. *Annu Rev Phys Chem* **1975**, *26* (1), 359–380. <https://doi.org/10.1146/annurev.pc.26.100175.002043>.
- (58) McLACHLAN, A. D.; BALL, M. A. Time-Dependent Hartree—Fock Theory for Molecules. *Rev Mod Phys* **1964**, *36* (3), 844–855. <https://doi.org/10.1103/RevModPhys.36.844>.
- (59) Chernyak, V.; Mukamel, S. Density-Matrix Representation of Nonadiabatic Couplings in Time-Dependent Density Functional (TDDFT) Theories. *J Chem Phys* **2000**, *112* (8), 3572–3579. <https://doi.org/10.1063/1.480511>.
- (60) Tommasini, M.; Chernyak, V.; Mukamel, S. Electronic Density-Matrix Algorithm for Nonadiabatic Couplings in Molecular Dynamics Simulations. *Int J Quantum Chem* **2001**, *85* (4–5), 225–238. <https://doi.org/10.1002/qua.1528>.
- (61) Furche, F. On the Density Matrix Based Approach to Time-Dependent Density Functional Response Theory. *J Chem Phys* **2001**, *114* (14), 5982–5992. <https://doi.org/10.1063/1.1353585>.
- (62) Furche, F.; Ahlrichs, R. Adiabatic Time-Dependent Density Functional Methods for Excited State Properties. *J Chem Phys* **2002**, *117* (16), 7433–7447. <https://doi.org/10.1063/1.1508368>.
- (63) Tretiak, S.; Chernyak, V. Resonant Nonlinear Polarizabilities in the Time-Dependent Density Functional Theory. *J Chem Phys* **2003**, *119* (17), 8809–8823. <https://doi.org/10.1063/1.1614240>.
- (64) Clark, J.; Nelson, T.; Tretiak, S.; Cirmi, G.; Lanzani, G. Femtosecond Torsional Relaxation. *Nature Physics* **2012**, *8* (3), 225–231. <https://doi.org/10.1038/nphys2210>.
- (65) Oldani, N.; Tretiak, S.; Bazan, G.; Fernandez-Alberti, S. Modeling of Internal Conversion in Photoexcited Conjugated Molecular Donors Used in Organic Photovoltaics. *Energy Environ Sci* **2014**, *7* (3), 1175. <https://doi.org/10.1039/c3ee43170c>.
- (66) Ondarse-Alvarez, D.; Oldani, N.; Tretiak, S.; Fernandez-Alberti, S. Computational Study of Photoexcited Dynamics in Bichromophoric Cross-Shaped Oligofluorene. *J Phys Chem A* **2014**, *118* (45), 10742–10753. <https://doi.org/10.1021/jp504720n>.
- (67) Alfonso Hernandez, L.; Nelson, T.; Gelin, M. F.; Lupton, J. M.; Tretiak, S.; Fernandez-Alberti, S. Interference of Interchromophoric Energy-Transfer Pathways in  $\pi$ -Conjugated Macrocycles. *Journal of Physical Chemistry Letters* **2016**, *7* (23), 4936–4944. <https://doi.org/10.1021/acs.jpcllett.6b02236>.
- (68) Sifain, A. E.; Bjorgaard, J. A.; Nelson, T. R.; Nebgen, B. T.; White, A. J.; Gifford, B. J.; Gao, D. W.; Prezhdo, O. V.; Fernandez-Alberti, S.; Roitberg, A. E.; Tretiak, S. Photoexcited Nonadiabatic Dynamics of Solvated Push–Pull  $\pi$ -Conjugated Oligomers with the NEXMD

- Software. *J Chem Theory Comput* **2018**, *14* (8), 3955–3966.  
<https://doi.org/10.1021/acs.jctc.8b00103>.
- (69) Ondarse-Alvarez, D.; Nelson, T.; Lupton, J. M.; Tretiak, S.; Fernandez-Alberti, S. Let Digons Be Bygones: The Fate of Excitons in Curved  $\pi$ -Systems. *J Phys Chem Lett* **2018**, *9* (24), 7123–7129. <https://doi.org/10.1021/acs.jpcllett.8b03160>.
- (70) Mukazhanova, A.; Negrin-Yuvero, H.; Freixas, V. M.; Tretiak, S.; Fernandez-Alberti, S.; Sharifzadeh, S. The Impact of Stacking and Phonon Environment on Energy Transfer in Organic Chromophores: Computational Insights. *J Mater Chem C Mater* **2023**, *11* (16), 5297–5306. <https://doi.org/10.1039/D3TC00479A>.
- (71) Ondarse-Alvarez, D.; Kömürlü, S.; Roitberg, A. E.; Pierdominici-Sottile, G.; Tretiak, S.; Fernandez-Alberti, S.; Kleiman, V. D. Ultrafast Electronic Energy Relaxation in a Conjugated Dendrimer Leading to Inter-Branch Energy Redistribution. *Physical Chemistry Chemical Physics* **2016**, *18* (36), 25080–25089. <https://doi.org/10.1039/C6CP04448D>.
- (72) Galindo, J. F.; Atas, E.; Altan, A.; Kuroda, D. G.; Fernandez-Alberti, S.; Tretiak, S.; Roitberg, A. E.; Kleiman, V. D. Dynamics of Energy Transfer in a Conjugated Dendrimer Driven by Ultrafast Localization of Excitations. *J Am Chem Soc* **2015**, *137* (36), 11637–11644. <https://doi.org/10.1021/jacs.5b04075>.
- (73) Fernandez-Alberti, S.; Roitberg, A. E.; Kleiman, V. D.; Nelson, T.; Tretiak, S. Shishiodoshi Unidirectional Energy Transfer Mechanism in Phenylene Ethynylene Dendrimers. *J Chem Phys* **2012**, *137* (22), 22A526. <https://doi.org/10.1063/1.4745835>.
- (74) Soler, M. A.; Roitberg, A. E.; Nelson, T.; Tretiak, S.; Fernandez-Alberti, S. Analysis of State-Specific Vibrations Coupled to the Unidirectional Energy Transfer in Conjugated Dendrimers. *J Phys Chem A* **2012**, *116* (40), 9802–9810. <https://doi.org/10.1021/jp301293e>.
- (75) Ondarse-Alvarez, D.; Oldani, N.; Roitberg, A. E.; Kleiman, V.; Tretiak, S.; Fernandez-Alberti, S. Energy Transfer and Spatial Scrambling of an Exciton in a Conjugated Dendrimer. *Physical Chemistry Chemical Physics* **2018**, *20* (47), 29648–29660. <https://doi.org/10.1039/C8CP05852K>.
- (76) Freixas, V. M. M.; Ondarse-Alvarez, D.; Tretiak, S.; Makhov, D. V. V.; Shalashilin, D. V. V.; Fernandez-Alberti, S. Photoinduced Non-Adiabatic Energy Transfer Pathways in Dendrimer Building Blocks. *J Chem Phys* **2019**, *150* (12), 124301. <https://doi.org/10.1063/1.5086680>.
- (77) Bonilla, V.; Freixas, V. M.; Fernandez-Alberti, S.; Galindo, J. F. Impact of the Core on the Inter-Branch Exciton Exchange in Dendrimers. *Physical Chemistry Chemical Physics* **2023**, *25* (17), 12097–12106. <https://doi.org/10.1039/D2CP06009D>.
- (78) Franklin-Mergarejo, R.; Nelson, T.; Tretiak, S.; Fernandez-Alberti, S. Phonon Bottleneck and Long-Lived Excited States in  $\pi$ -Conjugated Pyrene Hoop. *Physical Chemistry Chemical Physics* **2017**, *19* (14), 9478–9484. <https://doi.org/10.1039/C7CP00094D>.
- (79) Oldani, N.; Doorn, S. K.; Tretiak, S.; Fernandez-Alberti, S. Photoinduced Dynamics in Cycloparaphenylenes: Planarization, Electron–Phonon Coupling, Localization and Intra-Ring Migration of the Electronic Excitation. *Physical Chemistry Chemical Physics* **2017**, *19* (45), 30914–30924. <https://doi.org/10.1039/C7CP06426H>.
- (80) Rodríguez-Hernández, B.; Ondarse-Álvarez, D.; Oldani, N.; Martínez-Mesa, A.; Uranga-Piña, L.; Tretiak, S.; Fernández-Alberti, S. Modification of Optical Properties and Excited-

- State Dynamics by Linearizing Cyclic Paraphenylene Chromophores. *Journal of Physical Chemistry C* **2018**, *122* (29), 16639–16648.  
[https://doi.org/10.1021/ACS.JPCC.8B05582/SUPPL\\_FILE/JP8B05582\\_SI\\_005.MPG](https://doi.org/10.1021/ACS.JPCC.8B05582/SUPPL_FILE/JP8B05582_SI_005.MPG).
- (81) Franklin-Mergarejo, R.; Alvarez, D. O.; Tretiak, S.; Fernandez-Alberti, S. Carbon Nanorings with Inserted Acenes: Breaking Symmetry in Excited State Dynamics. *Scientific Reports* **2016**, *6* (1), 1–11. <https://doi.org/10.1038/srep31253>.
- (82) Freixas, V. M.; Tretiak, S.; Fernandez-Alberti, S. Infinitene: Computational Insights from Nonadiabatic Excited State Dynamics. *J Phys Chem Lett* **2022**, 8495–8501.  
<https://doi.org/10.1021/ACS.JPCLETT.2C02296>.
- (83) Negrin-Yuvero, H.; Freixas, V. M.; Ondarse-Alvarez, D.; Ledesma, A. E.; Tretiak, S.; Fernandez-Alberti, S. Photoexcited Energy Relaxation in a Zigzag Carbon Nanobelt. *The Journal of Physical Chemistry C* **2023**, *127* (11), 5449–5456.  
<https://doi.org/10.1021/acs.jpcc.2c08676>.
- (84) Zheng, F.; Fernandez-Alberti, S.; Tretiak, S.; Zhao, Y. Photoinduced Intra- and Intermolecular Energy Transfer in Chlorophyll a Dimer. *J Phys Chem B* **2017**, *121* (21), 5331–5339. <https://doi.org/10.1021/acs.jpcc.7b02021>.
- (85) Greenfield, M. T.; McGrane, S. D.; Bolme, C. A.; Bjorgaard, J. A.; Nelson, T. R.; Tretiak, S.; Scharff, R. J. Photoactive High Explosives: Linear and Nonlinear Photochemistry of Petrin Tetrazine Chloride. *J Phys Chem A* **2015**, *119* (20), 4846–4855.  
<https://doi.org/10.1021/acs.jpca.5b02092>.
- (86) Nelson, T.; Bjorgaard, J.; Greenfield, M.; Bolme, C.; Brown, K.; McGrane, S.; Scharff, R. J.; Tretiak, S. Ultrafast Photodissociation Dynamics of Nitromethane. *J Phys Chem A* **2016**, *120* (4), 519–526. <https://doi.org/10.1021/acs.jpca.5b09776>.
- (87) Lystrom, L.; Zhang, Y.; Tretiak, S.; Nelson, T. Site-Specific Photodecomposition in Conjugated Energetic Materials. *J Phys Chem A* **2018**, *122* (29), 6055–6061.  
<https://doi.org/10.1021/acs.jpca.8b04381>.
- (88) Freixas, V. M.; White, A. J.; Nelson, T.; Song, H.; Makhov, D. V.; Shalashilin, D.; Fernandez-Alberti, S.; Tretiak, S. Nonadiabatic Excited-State Molecular Dynamics Methodologies: Comparison and Convergence. *J Phys Chem Lett* **2021**, *12* (11), 2970–2982.  
<https://doi.org/10.1021/acs.jpcclett.1c00266>.
- (89) Negrin-Yuvero, H.; Freixas, V. M.; Rodriguez-Hernandez, B.; Rojas-Lorenzo, G.; Tretiak, S.; Bastida, A.; Fernandez-Alberti, S. Photoinduced Dynamics with Constrained Vibrational Motion: FrozeNM Algorithm. *J Chem Theory Comput* **2020**, *16* (12), 7289–7298.  
<https://doi.org/10.1021/acs.jctc.0c00930>.
- (90) Negrin-Yuvero, H.; Freixas, V. M.; Ondarse-Alvarez, D.; Alfonso-Hernandez, L.; Rojas-Lorenzo, G.; Bastida, A.; Tretiak, S.; Fernandez-Alberti, S. Vibrational Funnel for Energy Transfer in Organic Chromophores. *J Phys Chem Lett* **2023**, 4673–4681.  
<https://doi.org/10.1021/acs.jpcclett.3c00748>.
- (91) Walker, R. C.; Crowley, M. F.; Case, D. A. The Implementation of a Fast and Accurate QM/MM Potential Method in Amber. *J Comput Chem* **2008**, *29* (7), 1019–1031.  
<https://doi.org/10.1002/jcc.20857>.
- (92) Dewar, M. J. S.; Zoebisch, E. G.; Healy, E. F.; Stewart, J. J. P. Development and Use of Quantum Mechanical Molecular Models. 76. AM1: A New General Purpose Quantum

- Mechanical Molecular Model. *J Am Chem Soc* **1985**, *107* (13), 3902–3909. <https://doi.org/10.1021/ja00299a024>.
- (93) Stewart, J. J. P. Optimization of Parameters for Semiempirical Methods I. Method. *J Comput Chem* **1989**, *10* (2), 209–220. <https://doi.org/10.1002/jcc.540100208>.
- (94) Stewart, J. J. P. Optimization of Parameters for Semiempirical Methods V: Modification of NDDO Approximations and Application to 70 Elements. *J Mol Model* **2007**, *13* (12), 1173–1213. <https://doi.org/10.1007/S00894-007-0233-4/FIGURES/10>.
- (95) Davidson, E. R. *Reduced Density Matrices in Quantum Chemistry*; Academic Press, New York, 1976.
- (96) Tretiak, S.; Mukamel, S. Density Matrix Analysis and Simulation of Electronic Excitations in Conjugated and Aggregated Molecules. *Chem Rev* **2002**, *102* (9), 3171–3212. <https://doi.org/10.1021/cr0101252>.
- (97) Mukamel, S. Electronic Coherence and Collective Optical Excitations of Conjugated Molecules. *Science (1979)* **1997**, *277* (5327), 781–787. <https://doi.org/10.1126/science.277.5327.781>.
- (98) Mukamel, S. *Principles of Nonlinear Optical Spectroscopy*; Oxford University Press.
- (99) Davidson, E. R. The Iterative Calculation of a Few of the Lowest Eigenvalues and Corresponding Eigenvectors of Large Real-Symmetric Matrices. *J Comput Phys* **1975**, *17* (1), 87–94. [https://doi.org/10.1016/0021-9991\(75\)90065-0](https://doi.org/10.1016/0021-9991(75)90065-0).
- (100) Tavernelli, I.; Curchod, B. F. E.; Laktionov, A.; Rothlisberger, U. Nonadiabatic Coupling Vectors for Excited States within Time-Dependent Density Functional Theory in the Tamm–Dancoff Approximation and Beyond. *J Chem Phys* **2010**, *133* (19), 194104. <https://doi.org/10.1063/1.3503765>.
- (101) Stratmann, R. E.; Scuseria, G. E.; Frisch, M. J. An Efficient Implementation of Time-Dependent Density-Functional Theory for the Calculation of Excitation Energies of Large Molecules. *J Chem Phys* **1998**, *109* (19), 8218. <https://doi.org/10.1063/1.477483>.
- (102) Chernyak, V.; Schulz, M. F.; Mukamel, S.; Tretiak, S.; Tsiper, E. V. Krylov-Space Algorithms for Time-Dependent Hartree–Fock and Density Functional Computations. *J Chem Phys* **2000**, *113* (1), 36–43. <https://doi.org/10.1063/1.481770>.
- (103) Tretiak, S. S.; Isborn, C. M. M.; Niklasson, A. M. N. N.; Challacombe, M. Representation Independent Algorithms for Molecular Response Calculations in Time-Dependent Self-Consistent Field Theories. *J Chem Phys* **2009**, *130* (5), 054111. <https://doi.org/10.1063/1.3068658>.
- (104) Crespo-Otero, R.; Barbatti, M. Recent Advances and Perspectives on Nonadiabatic Mixed Quantum-Classical Dynamics. *Chem Rev* **2018**, *118* (15), 7026–7068. <https://doi.org/10.1021/acs.chemrev.7b00577>.
- (105) Barbatti, M.; Aquino, A. J. A.; Szymczak, J. J.; Nachtigallová, D.; Hobza, P.; Lischka, H. Relaxation Mechanisms of UV-Photoexcited DNA and RNA Nucleobases. *Proc Natl Acad Sci U S A* **2010**. <https://doi.org/10.1073/pnas.1014982107>.
- (106) Nelson, T.; Fernandez-Alberti, S.; Roitberg, A. E.; Tretiak, S. Electronic Delocalization, Vibrational Dynamics, and Energy Transfer in Organic Chromophores. *J Phys Chem Lett* **2017**, *8* (13), 3020–3031. <https://doi.org/10.1021/acs.jpcllett.7b00790>.

- (107) Zobel, J. P.; González, L. The Quest to Simulate Excited-State Dynamics of Transition Metal Complexes. *JACS Au* **2021**, *1* (8), 1116–1140. <https://doi.org/10.1021/jacsau.1c00252>.
- (108) Nijjar, P.; Jankowska, J.; Prezhdo, O. V. Ehrenfest and Classical Path Dynamics with Decoherence and Detailed Balance. *J Chem Phys* **2019**, *150* (20), 204124. <https://doi.org/10.1063/1.5095810>.
- (109) Nam, Y.; Song, H.; Freixas, V. M.; Keefer, D.; Fernandez-Alberti, S.; Lee, J. Y.; Garavelli, M.; Tretiak, S.; Mukamel, S. Monitoring Vibronic Coherences and Molecular Aromaticity in Photoexcited Cyclooctatetraene with an X-Ray Probe: A Simulation Study. *Chem Sci* **2023**, *14* (11), 2971–2982. <https://doi.org/10.1039/D2SC04335A>.
- (110) Tully, J. C. Molecular Dynamics with Electronic Transitions. *J Chem Phys* **1990**, *93* (2), 1061–1071. <https://doi.org/10.1063/1.459170>.
- (111) Nelson, T.; Fernandez-Alberti, S.; Chernyak, V.; Roitberg, A. E.; Tretiak, S. Nonadiabatic Excited-State Molecular Dynamics Modeling of Photoinduced Dynamics in Conjugated Molecules. *J Phys Chem B* **2011**, *115* (18), 5402–5414. <https://doi.org/10.1021/jp109522g>.
- (112) Nelson, T.; Fernandez-Alberti, S.; Roitberg, A. E.; Tretiak, S. Nonadiabatic Excited-State Molecular Dynamics: Treatment of Electronic Decoherence. *J Chem Phys* **2013**, *138* (22), 224111. <https://doi.org/10.1063/1.4809568>.
- (113) Fernandez-alberti, S.; Roitberg, A. E.; Nelson, T.; Tretiak, S. Identification of Unavoided Crossings in Nonadiabatic Photoexcited Dynamics Involving Multiple Electronic States in Polyatomic Conjugated Molecules. *J Chem Phys* **2012**, *137* (1), 014512. <https://doi.org/10.1063/1.4732536>.
- (114) Thompson, A. L.; Punwong, C.; Martínez, T. J. Optimization of Width Parameters for Quantum Dynamics with Frozen Gaussian Basis Sets. *Chem Phys* **2010**, *370* (1–3), 70–77. <https://doi.org/10.1016/j.chemphys.2010.03.020>.
- (115) Born, Max; Huang, K. *Dynamical Theory of Crystal Lattices*; Oxford University Press: London, New York, 1954.
- (116) Makhov, D. V.; Glover, W. J.; Martinez, T. J.; Shalashilin, D. V. Ab Initio Multiple Cloning Algorithm for Quantum Nonadiabatic Molecular Dynamics. *J Chem Phys* **2014**, *141* (5), 054110. <https://doi.org/10.1063/1.4891530>.
- (117) Ben-Nun, M.; Quenneville, J.; Martínez, T. J. Ab Initio Multiple Spawning: Photochemistry from First Principles Quantum Molecular Dynamics. *J Phys Chem A* **2000**, *104* (22), 5161–5175. <https://doi.org/10.1021/jp994174i>.
- (118) Curchod, B. F. E.; Martínez, T. J. Ab Initio Nonadiabatic Quantum Molecular Dynamics. *Chem Rev* **2018**, *118* (7), 3305–3336. <https://doi.org/10.1021/acs.chemrev.7b00423>.
- (119) Paterlini, M. G.; Ferguson, D. M. Constant Temperature Simulations Using the Langevin Equation with Velocity Verlet Integration. *Chem Phys* **1998**, *236* (1–3), 243–252. [https://doi.org/10.1016/S0301-0104\(98\)00214-6](https://doi.org/10.1016/S0301-0104(98)00214-6).
- (120) Park, Y. Il; Kuo, C.-Y.; Martinez, J. S.; Park, Y.-S.; Postupna, O.; Zhugayevych, A.; Kim, S.; Park, J.; Tretiak, S.; Wang, H.-L. Tailored Electronic Structure and Optical Properties of Conjugated Systems through Aggregates and Dipole–Dipole Interactions. *ACS Appl Mater Interfaces* **2013**, *5* (11), 4685–4695. <https://doi.org/10.1021/am400766w>.

- (121) Cramer, C. J.; Truhlar, D. G. Implicit Solvation Models: Equilibria, Structure, Spectra, and Dynamics. *Chem Rev* **1999**, *99* (8), 2161–2200. <https://doi.org/10.1021/cr960149m>.
- (122) Nelson, T.; Fernandez-Alberti, S.; Roitberg, A. E.; Tretiak, S. Artifacts Due to Trivial Unavoided Crossings in the Modeling of Photoinduced Energy Transfer Dynamics in Extended Conjugated Molecules. *Chem Phys Lett* **2013**, *590*, 208–213. <https://doi.org/10.1016/j.cplett.2013.10.052>.
- (123) Soler, M. A.; Bastida, A.; Farag, M. H.; Zúñiga, J.; Requena, A. A Method for Analyzing the Vibrational Energy Flow in Biomolecules in Solution. *J Chem Phys* **2011**, *135* (20), 204106. <https://doi.org/10.1063/1.3663707>.
- (124) Rodríguez-Hernández, B.; Oldani, N.; Martínez-Mesa, A.; Uranga-Piña, L.; Tretiak, S.; Fernandez-Alberti, S. Photoexcited Energy Relaxation and Vibronic Couplings in  $\pi$ -Conjugated Carbon Nanorings. *Physical Chemistry Chemical Physics* **2020**, *22* (27), 15321–15332. <https://doi.org/10.1039/D0CP01452D>.
- (125) Freixas, V. M.; Wilhelm, P.; Nelson, T.; Hinderer, F.; Höger, S.; Tretiak, S.; Lupton, J. M.; Fernandez-Alberti, S. Excitation Energy Transfer between Bodipy Dyes in a Symmetric Molecular Excitonic Seesaw. *J Phys Chem A* **2021**, *125* (38), 8404–8416. <https://doi.org/10.1021/acs.jpca.1c06332>.
- (126) Nelson, T.; Naumov, A.; Fernandez-Alberti, S.; Tretiak, S. Nonadiabatic Excited-State Molecular Dynamics: On-the-Fly Limiting of Essential Excited States. *Chem Phys* **2016**, *481*, 84–90. <https://doi.org/10.1016/j.chemphys.2016.05.017>.
- (127) Soler, M. A.; Nelson, T.; Roitberg, A. E.; Tretiak, S.; Fernandez-Alberti, S. Signature of Nonadiabatic Coupling in Excited-State Vibrational Modes. *J Phys Chem A* **2014**, *118* (45), 10372–10379. <https://doi.org/10.1021/jp503350k>.
- (128) Andersen, H. C. Rattle: A “Velocity” Version of the Shake Algorithm for Molecular Dynamics Calculations. *J Comput Phys* **1983**, *52* (1), 24–34. [https://doi.org/10.1016/0021-9991\(83\)90014-1](https://doi.org/10.1016/0021-9991(83)90014-1).
- (129) Mai, S.; Marquetand, P.; González, L. Surface Hopping Molecular Dynamics. In *Quantum Chemistry and Dynamics of Excited States*; Wiley, 2020; pp 499–530. <https://doi.org/10.1002/9781119417774.ch16>.
- (130) McSloy, A.; Fan, G.; Sun, W.; Hölzer, C.; Friede, M.; Ehlert, S.; Schütte, N.-E.; Grimme, S.; Frauenheim, T.; Aradi, B. TBMaLT, a Flexible Toolkit for Combining Tight-Binding and Machine Learning. *J Chem Phys* **2023**, *158* (3), 034801. <https://doi.org/10.1063/5.0132892>.
- (131) Zhou, G.; Lubbers, N.; Barros, K.; Tretiak, S.; Nebgen, B. Deep Learning of Dynamically Responsive Chemical Hamiltonians with Semiempirical Quantum Mechanics. *Proceedings of the National Academy of Sciences* **2022**, *119* (27). <https://doi.org/10.1073/pnas.2120333119>.
- (132) Goldman, N.; Fried, L. E.; Lindsey, R. K.; Pham, C. H.; Dettori, R. Enhancing the Accuracy of Density Functional Tight Binding Models Through ChIMES Many-Body Interaction Potentials. **2023**.
- (133) Kulik, H. J.; Hammerschmidt, T.; Schmidt, J.; Botti, S.; Marques, M. A. L.; Boley, M.; Scheffler, M.; Todorović, M.; Rinke, P.; Oses, C.; Smolyanyuk, A.; Curtarolo, S.; Tkatchenko, A.; Bartók, A. P.; Manzhos, S.; Ihara, M.; Carrington, T.; Behler, J.; Isayev, O.; Veit, M.; Grisafi, A.; Nigam, J.; Ceriotti, M.; Schütt, K. T.; Westermayr, J.; Gastegger, M.;

Maurer, R. J.; Kalita, B.; Burke, K.; Nagai, R.; Akashi, R.; Sugino, O.; Hermann, J.; Noé, F.; Pilati, S.; Draxl, C.; Kuban, M.; Rigamonti, S.; Scheidgen, M.; Esters, M.; Hicks, D.; Toher, C.; Balachandran, P. V; Tamblyn, I.; Whitlam, S.; Bellinger, C.; Ghiringhelli, L. M. Roadmap on Machine Learning in Electronic Structure. *Electronic Structure* **2022**, 4 (2), 023004. <https://doi.org/10.1088/2516-1075/ac572f>.